TIME-DEPENDENT INITIATION OF MULTIPLE HYDRAULIC FRACTURES IN ROCKS

by

Uwaifo Efosa Christopher

B.Eng in Chemical Engineering, University of Benin, Nigeria 2010

Submitted to the Graduate Faculty of

Swanson School of Engineering in partial fulfillment

of the requirement of the degree of

Master of Science

University of Pittsburgh

2015

UNIVERSITY OF PITTSBURGH

SWANSON SCHOOL OF ENGINEERING

This thesis was presented

by

Uwaifo Efosa Christopher

It was defended on

November 11, 2015

and approved by

Andrew P. Bunger, PhD, Assistant Professor

Badie I. Morsi, PhD, Professor

Sinisha A. Jikich, PhD, Adjunct Professor

Thesis Advisor: Andrew P. Bunger, PhD, Assistant Professor

TIME-DEPENDENT INITIATION OF HYDRAULIC FRACTURES IN ROCKS.

Uwaifo Efosa Christopher, M.S

University of Pittsburgh, 2015

The challenge of creating multiple hydraulic fractures in petroleum reservoirs is approached by experimentally observing the time-dependence of the hydraulic fracture initiation/breakdown under different cases of fluid penetration into the rock during fracture initiation, and confining stresses.

The objective is to validate the plane-strain models of breakdown pressure for sandstone and granite. A comparison of cases of no-fluid penetration by using a jacketed wellbore, partial fluid penetration using soybean oil and glycerin, and full penetration using water was performed and the pressures required to create instantaneous and delayed breakdown, in cases of zero, low and moderate confining stresses recorded. In each case, the relationship between pressure and time to failure is compared with theory.

Experimental results show strong agreement with theory in the form of a predictable exponential relationship between time to breakdown and the wellbore pressure. Furthermore, the results enable experimentally derived values of β, a parameter varying from 1-2 for zero and full fluid penetration, respectively. By comparing values for soybean oil, glycerin, and water the dependence of β on viscosity is readily observed. The importance of β is further highlighted by

the ability to achieve breakdown after 500 seconds with only 25% of the tensile strength of the rock when $\beta=2$.

In summary, the main contributions are: 1) The first experimental validation of the predictable exponential relationship between time to initiation/breakdown of hydraulic fractures with wellbore pressure, 2) Experimental quantification of the role of fluid penetration, providing one of the clearest validations of classical hydraulic fracture breakdown models, 3) The first experimental demonstration of the role of confining stress on delayed hydraulic fracture initiation/breakdown, validating theory in the case of finite fluid penetration and demonstrating the need for further modeling in the case of zero fluid penetration.

TABLE OF CONTENTS

LIST OF TABLES

LIST OF FIGURES

ACKNOWLEDGEMENTS AND DEDICATION

I would like to specifically show my gratitude to:

God, for everything.

My family, especially my parents Mr. & Mrs. E.O Uwaifo, for their unfailing love.

My research advisor Dr. Andrew Bunger for his time and energy in supervising this work.

My academic advisor Dr. Badie Morsi, for his fatherly advice and support to me.

Dr. Sinisha Jikich for his academic, career and research advice.

The students in the Hydraulic Fracturing Group at University of Pittsburgh, especially Guanyi Lu and Brandon Ames, for our collaborative discussions and work. Dr. Romain Prioul & team at Schlumberger Doll Research are also acknowledged.

Charles ‘Scooter’ Hager, for his help with equipment training, operation and maintenance

My friends at Chi Alpha, for being a strong support group for me.

Dr. Sola Talabi, for his mentorship. Dr Sylvanus Wosu is also gratefully acknowledged.

Dr. Samuel Ogbeide, Dr. Anslem Igbafe, Dr. Andrew Odeh and Mr. Femi Bajomo for the strong engineering background they helped me develop before my graduate degree.

My friends, especially Juliann ‘Jules’ Hudak, for their friendship and support. Todd & Minerva Morrow, Arabia & Quintin Littlejohn are also appreciated.

My classmates and friends at Pitt are also gratefully acknowledged.

Finally, I would like to give credit where it is due, and dedicate this work to Mrs. Genevieve Littlejohn, who met me a lost stranger on my first day in America, and has become a mother to me. And to Ella, my newborn niece I long to hold in my arms.

1.0 INTRODUCTION

Hydraulic fracturing is a production optimization and stimulation strategy whose initial application was to reduce skin effect in conventional reservoirs including the bypass of near wellbore damage caused by, for example, reservoir fines and drilling mud residue. However, the US energy crisis of 1970s led to increased focus on unconventional resources, and further developments in horizontal drilling led to hydraulic fracturing being used to produce hydrocarbons from low permeability ("tight") formations such as oil and gas bearing shale (Nolte, 2000).

Application of hydraulic fracturing to shale reservoir stimulation involves drilling through the formation with a horizontal section usually in thousands of feet, creating small holes in the casing known as perforation clusters, and then pumping fluid downhole at high pressure and high flowrate to create fractures. Typically fluid is injected to 3-6 clusters at the same time in each so-called "stage", and the desire is to generate a hydraulic fracture from each cluster.

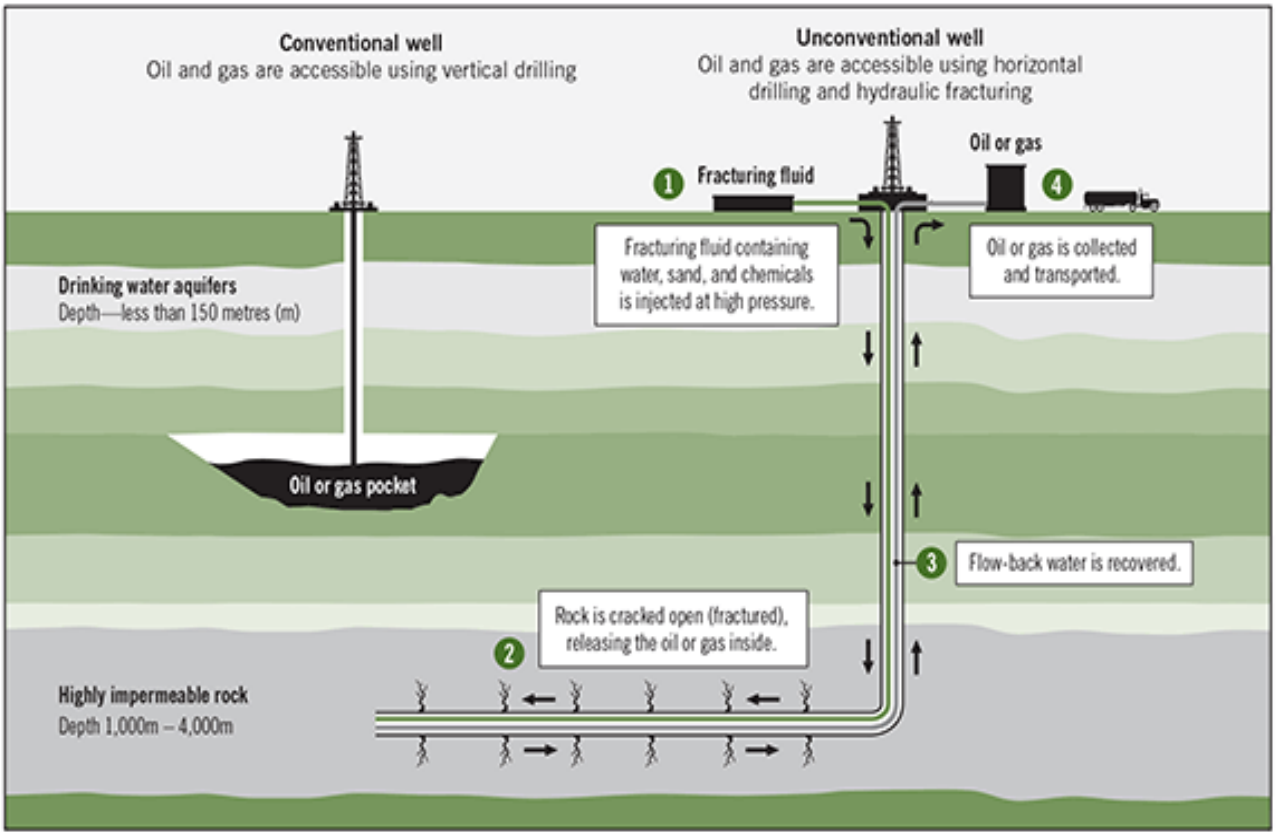

Figure 1: A pictorial description of hydraulic fracturing (Source http://www.oag-bvg.gc.ca)

1.1 PROBLEM STATEMENT

Because most tight formations will remain uneconomic to produce without hydraulic fracturing, the success of the fracturing operation is critical. Obviously, the more fractures are initiated, the more fractures are able to grow. The more fractures that grow, the more the stimulated reservoir volume, and hence the more hydrocarbon production can be produced.

Therefore, a vital question is: Is it possible to have multiple initiation of hydraulic fractures within a stage containing multiple perforation clusters when variability of the reservoir properties (mainly the minimum stress) insures that all clusters cannot initiate hydraulic fractures

simultaneously? In other words, what are the mechanism(s) by which hydraulic fractures can be initiated once one fracture has already started growing and the wellbore pressure is therefore no longer increasing? A correlated and practically-important question is what are the conditions that favor multiple initiation of hydraulic fractures?

An important note about the theory and experimental design is in order. While the inspiration for this study is for 'transverse' hydraulic fracture initiation from horizontal wells (i.e. orthogonal to the wellbore), here the theory and experiments are developed for stress conditions and fracture orientation typical of vertical wells, the so-called axial or longitudinal fractures. This is prudent because this situation will result in initiation parallel to the wellbore axis which is much easier to produce in the lab and capture using established theory. Furthermore, the basic questions discussed above can be well addressed using this simpler geometry analogous to a vertical wellbore. A future step will be to consider these conditions for horizontal wells.

1.2 APPROACH

One property of rocks that can be exploited to answer these questions is its capacity to fail after a period of time under sustained, sub-critical loadings. This property is commonly referred to as static fatigue (Zhurkov, 1984). For a heterogeneous rock, inevitably one fracture will initiate first and this will be accompanied by a peak in the pressure. This research is concerned with the remaining fractures, exploring the possibility of whether static fatigue of rock can lead to creation of additional fractures after a delayed time (and a sub-critical pressure condition unfavorable for instantaneous initiation/breakdown).

Importantly, we attempt to see if there is an obvious, predictable correlation between the applied pressure and 'delay time'. We apply the theory from Bunger and Lu (2015) and also study factors that control this process, such as viscosity-controlled fluid penetration into the rock prior to and during fracture initiation, the confining stresses, and a proposed property for quantifying static fatigue behavior (χ) relating the tensile stress required for breakage after a certain time to known tensile stress required for instantaneous breakdown.

1.3 OUTLINE OF DISSERTATION

Chapter Two starts with a rationale for optimizing hydraulic fracturing, and goes on to discuss the initiation phase of hydraulic fractures. How geo-mechanical rock property heterogeneity causes limited fracture initiations in a perforation cluster is also expounded, as are requirements for initiation of multiple fractures in a perforation cluster. Also provided is a theoretical explanation of 'delayed initiation', along with a description of each controlling parameter.

Chapter Three describes the different experiments carried out and shows the experimental set-ups. Also explained are the scientific reasoning behind the set-up design as well. The limitations of equipment used are also explained and photographic illustrations are also shown.

Chapter Four shows the results from the delayed breakdown experiments on sandstone and granite with different cases of fluid penetration and confining stress.

Chapter Five discusses the role of fluid penetration in time-dependent initiation of hydraulic fractures, and discusses the knowledge gleaned from experiment where fluid penetration is varied. Determination of the value of parameter β for select fluids is also undertaken, noting that

theoretically β varies from 1-2 for zero penetration and complete penetration of the fluid into the near wellbore region prior to fracture initiation, respectively. The relationship between β and fluid viscosity is also noted.

Chapter Six shows and discusses the role of confining stress in time-dependent initiation of hydraulic fractures by comparing cases of no-confinement to different values of confinement each in two dissimilar rocks – granite and sandstone.

Chapter Seven discusses the lessons learnt, summarizes our observations and conclusions and discusses potential further work on this topic.

2.0 LITERATURE REVIEW

2.1 WHY HYDRAULIC FRACTURING?

In this era where aquifer depletion, environmental pollution and rising CO_2 atmospheric levels are strong and legitimate concerns, why should hydraulic fracturing still be considered an important technology?

Firstly, because hydraulic fracturing can help nations achieve energy security. The EIA evaluated shale formations in 43 countries, including the United States, and estimated recoverable resources of 345 billion barrels of shale oil and 7,299 trillion cubic feet of shale gas. (EIA, 2015). These resources can ensure that countries independently produce the energy they need, thus guaranteeing economic stability.

Secondly, because natural gas, a ‘transition fuel’ is more environmentally friendly than coal, gasoline, fuel oil and diesel. Combustion of methane produces significantly less air pollutants and greenhouse gases compared to the above mentioned fuels. Admittedly, there are concerns over methane leaks during production and transportation – especially as methane has a high Global Warming Potential. Also, the adoption of a robust climate policy may be necessary to ensure its long term viability as a ‘bridge fuel’.

Thirdly because the petroleum industry is investing in sustainable procedures to reduce water usage, environmental pollution and degradation, which has been a substantial challenge to the

industry with profound importance also for public acceptance. The increasing reuse of flowback water in the Marcellus Shale is a good example (Yoxtheimer, 2013).

And fourthly because there is a current lack of economic alternatives - renewable energy is still developing, expensive and insufficient.

Optimizing hydraulic fracturing, by reducing its energy and environmental footprint is very important to its long term acceptability, and this study is one of many attempts to do that.

2.2 CONDITIONS FOR INITIATION OF HYDRAULIC FRACTURES

For a subsurface reservoir, the state of stress underground is such that there are three orthogonal stresses: one vertical stress and two horizontal stresses. The magnitude of these stresses are usually determined by tectonic conditions.

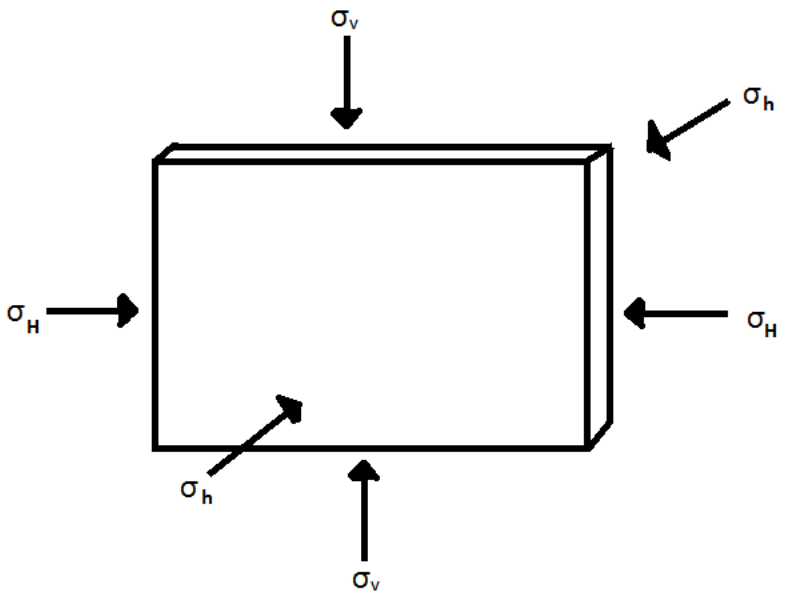

Figure 2. State of stress underground

According to Hubbert and Willis (1957), Haimson and Fairhurst (1967), Detorunay and Carbonell (1997), Bunger and Lu (2015), assuming plane-strain conditions for such a reservoir rock with pore pressure p_0, for a well drilled parallel to the vertical stress σ_v and pressurized by a wellbore pressure p_w, we can write the induced maximum normal tangential stress in the near wellbore region as

$$\sigma_{\theta\theta}^{(\max)} = \beta p_w - \hat{\sigma} \qquad (1)$$

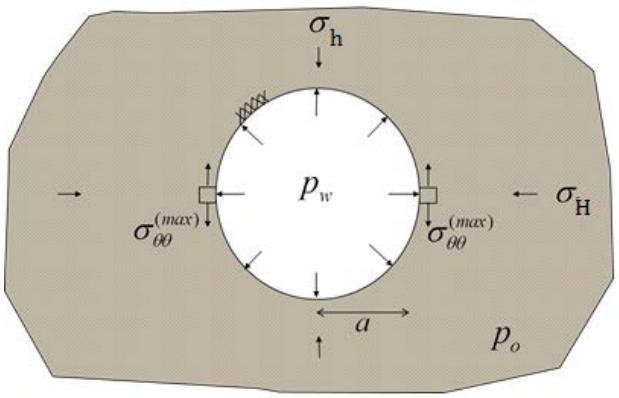

Figure 3: Stresses in a pressurized wellbore shown in a plane. From Bunger & Lu (2015)

where $\sigma_{\theta\theta}^{(max)}$ is the maximum normal tangential effective stress, also called the Terzaghi stress, induced by the fracturing fluid, p_w is the wellbore pressure, β is used to represent the degree of fluid penetration, its' value ranging from 1 in a no-penetration case to 2 in a full penetration case. This is further discussed in Section 2.5.2. Detournay and Carbonell (1997) and Bunger and Lu (2015) denote the case where there is no fluid penetration into the pores and flaws of the rock and the pressurization is 'fast' as following Hubbert and Willis' (1957) prediction. Here, β=1. The case where there is fluid penetration into the pores and flaws of the rock is called the 'slow' pressurization regime and $1 < \beta \leq 2$, with β approaching a value of 2 for a dry rock having no

rock-fluid coupling and having a Biot's co-efficient of zero. This follows Haimson and Fairhurst's (1967) prediction.

From Bunger and Lu (2015),

$$\beta = \begin{cases} 1, & H-W(\,fast) \\ 2(1-\eta), & H-F(slow) \end{cases} \qquad (2)$$

η is a poroelasticity constant whose range is $0 \leq \eta \leq 0.5$ and can be mathematically expressed as:

$$\eta = \frac{b(1-2\nu)}{2(1-\nu)} \qquad (3)$$

b is the Biot's coefficient and ν is Poisson's ratio of the rock. The last term $\hat{\sigma}$ in equation (1) is the confining stress term given by

$$\hat{\sigma} = \begin{cases} -\sigma_H + 3\sigma_h - p_0, & H-W(\,fast) \\ -\sigma_H + 3\sigma_h - 2\eta p_0, & H-F(slow) \end{cases} \qquad (4)$$

Where σ_H and σ_h are two horizontal stresses with $\sigma_H > \sigma_h$. We have assumed plane-strain conditions along the vertical direction, so σ_v is of no effect to the problem. p_0 denotes the in-situ pore pressure.

When the wellbore pressure is such that the maximum normal tangential stress it creates is equal to the tensile strength of a rock, a fracture is created. This pressure is typically called the initiation pressure. Often it nearly corresponds to the peak pressure, in which case approximates the so-called breakdown pressure. In the classical theories (Hubbert & Willis, 1957 and Haimson & Fairhurst, 1967), breakdown pressure is taken to be synonymous with initiation.

2.3 CONDITIONS FOR INITIATING ADDITIONAL FRACTURES AFTER BREAKDOWN

Consider a horizontal well that is to be fractured. The lateral portion of the well is sub-divided into sections called stages. Each stage contains, typically, 3-6, roughly 2-foot long clusters of perforations (‘perf’ clusters), with each perf cluster made up of individual perforations (holes). Traditionally, these clusters are placed by simple geometry – dividing the well section into equally spaced portions, although there is newer technology – engineered completions – that attempts to group perf clusters using their petrophysical and geo-mechanical properties (Walker et al, 2012).

Especially in geometric completions, because petroleum reservoir rocks are heterogeneous; within a single stage, there will be portions of fairly different tensile strengths. When fluid is pumped into all the perforation cluster simultaneously, (as shown in Figure 5), the first hydraulic fracture will initiate at the ‘weakest’ perforation – the one with the lowest tensile strength. If other perforations are of very similar tensile strength, then they will be fractured concurrently. However, it is unlikely to initiate fractures in all the perforations at the same time when their elastic moduli, minimum stress and tensile strengths are significantly varying.

The typical bottomhole net pressure record from a fracture operation in a stage is shown below

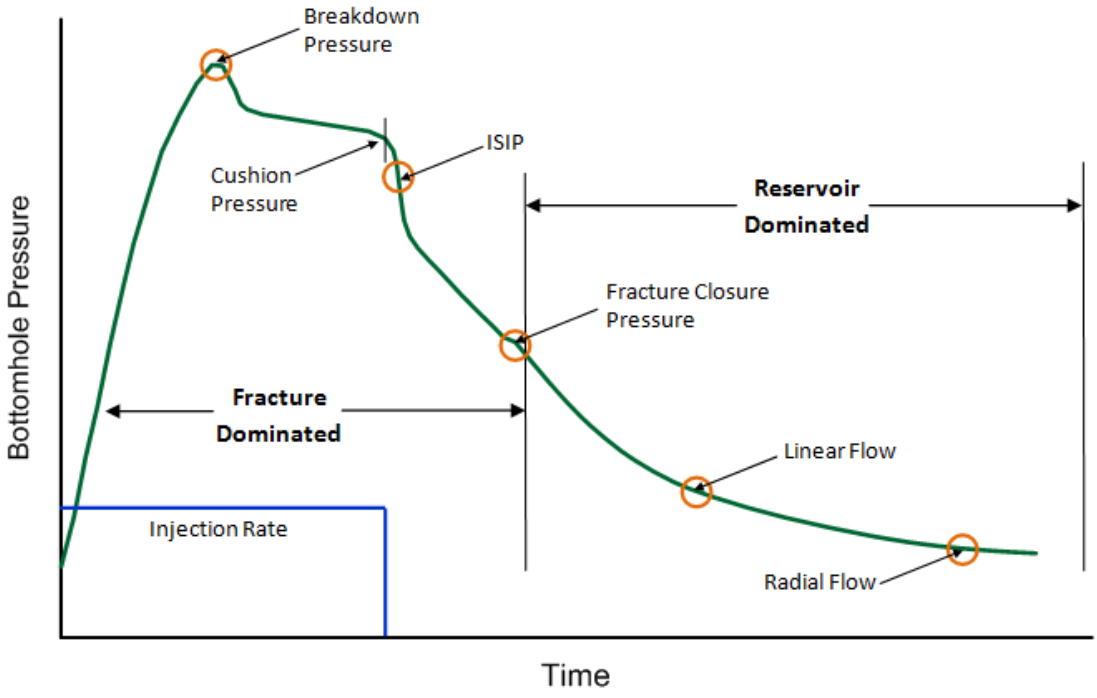

Figure 4: Typical bottomhole net pressure record during hydraulic fracturing operation. (Image Courtesy www.fekete.com)

Unless the pressure continues to increase after this first initiation, and this is not usually the case, the only other way to initiate additional fractures is for them to be initiated at lower pressures than required for instantaneous initiation. A look at Figure 4, and most bottom hole pressure records from fracturing operations, will show a period of fairly constant pressure period between the Breakdown Pressure (when the fracture is created) and the Instantaneous Shut In Pressure (ISIP). Since this pressure is insufficient to fracture the rock at other perforation points instantaneously, we explore if it can fracture them after a delayed time.

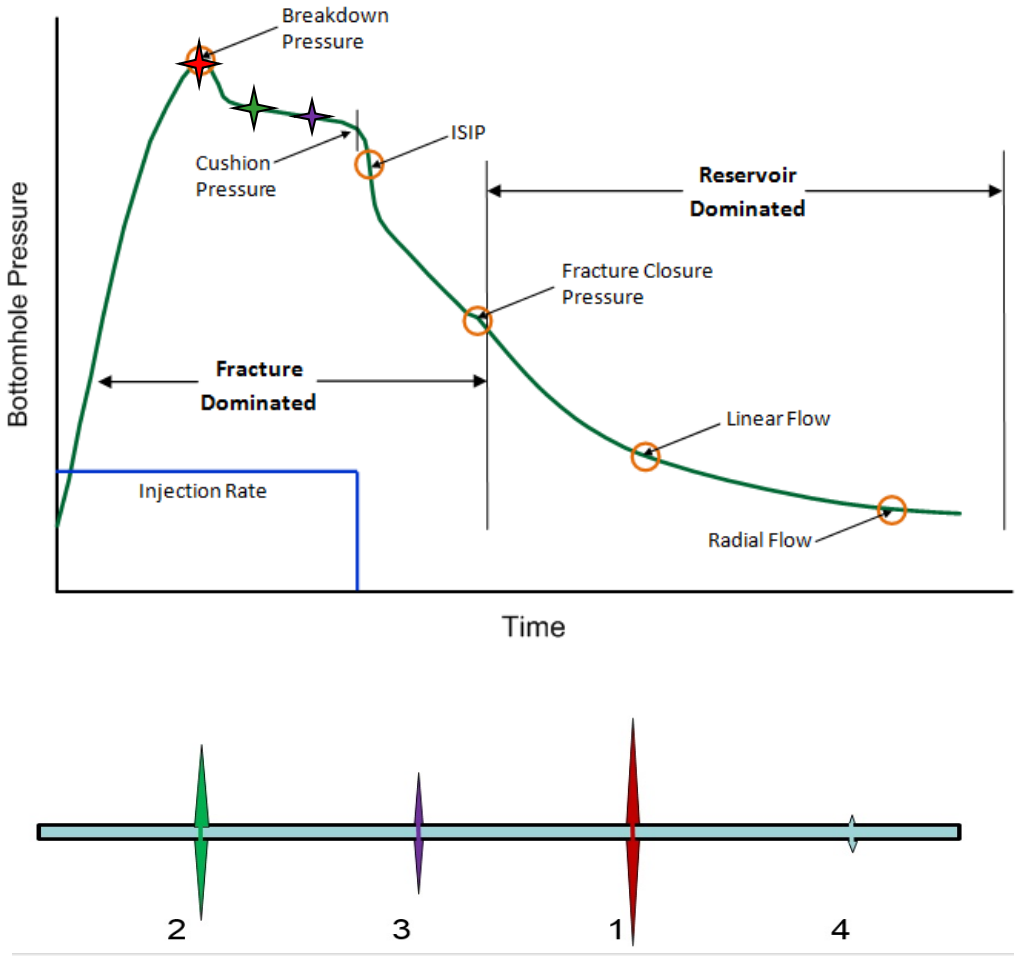

Figure 5: Delayed initiation of multiple hydraulic fractures (2, 3 then perhaps 4) after the first fracture (1) initiates instantaneously.

The gains from initiating multiple fractures, especially at sub-critical pressures, from a perforation cluster are numerous. More fractures mean a larger stimulated reservoir volume; hence fewer wells will have to be drilled or re-fractured for the same amount of hydrocarbons. This will lead to less environmental footprint, lower water consumption, lower costs, lower material and energy consumption. It is also important to state that the period we consider in this work, is the first phase of the fracturing operation, typically marked by the use of a pad fluid.

2.4 STATIC FATIGUE IN ROCKS

To understand how rocks can fail in a 'sub-critical', or 'delayed' manner, we begin with a general study of the material phenomenon called static fatigue. Zhurkov (1984) proposed a kinetic theory to explain how materials fail. He considered material failure as a 'time-process' that is dependent on the applied stress and material temperature and postulated a relationship that applied for all fifty of the materials he tested, shown below

$$t = t_0 \exp[(U_0 - \gamma\sigma)/kT] \quad (5)$$

where t_0 is the reciprocal of the natural oscillation frequency of atoms in solids, U_0 is the energy barrier determining the probability of breakage of the bonds responsible for strength, γ is a ratio of bond overstress to average material stress, σ is the applied tensile stress, k, is the Boltzmann's constant, and T is the absolute temperature.

Zhurkov's relationship tells us that at time t_o the material is damaged by the intrinsic atomic vibrations and no applied stress. This time typically approaches infinity for most materials. Also, Zhurkov neglects the atomic scale bond reforming; only bond breaking is considered. At very low stresses, bond breaking and re-forming are in equilibrium – and here, the validity of Zhurkov's theory wanes. However, in hydraulic fracturing, we are interested in creating delayed fractures at reasonable time scales of circa 1 – 1000 seconds.

We can rewrite equation 5 as

$$t = t_0 \exp(U_0/kT) * \exp[(-\gamma)\sigma_{\theta\theta}^{(max)}/kT] \quad (5a)$$

as the applied tensile stress in our case (eq 1) is $\sigma_{\theta\theta}^{(max)}$. We can also write

$$t = A * \exp[(-\gamma)\sigma_{\theta\theta}^{(max)}/kT] \quad (5b)$$

where A = $t_0 \exp(U_0 / kT)$

If we limit our observations to the applied stress and time to failure, and assume other parameters stay constant, like Kear and Bunger (2014) did in their experiments of flexure tests on crystalline gabbro rocks, an exponential relationship between these two parameters is predictable.

That is

$$t \propto \exp[\sigma_{\theta\theta}^{(max)}] \quad (5c)$$

We can also rewrite equation 5b as

$$t = A * \exp[(-\gamma) * (\beta P_w - \hat{\sigma})/kT] \quad (5d)$$

2.5 PARAMETER χ

Bunger and Lu (2015), following Kear and Bunger (2014) proposed a relationship around a hypothetical parameter χ viz,

$$\sigma_t(t_1) = (1 - \chi(t_0, t_1)) \cdot \sigma_t(t_0) \quad (6)$$

where $\sigma_t(t_0)$ and $\sigma_t(t_1)$ are the nominal tensile stress that will cause failure after time t_0 and $t_1$respectively. $\chi(t_0, t_1)$ is an experimentally determined parameter that represents the ratio of tensile stresses corresponding to two times to failure t_0 and t_1.

They used the static fatigue behavior observed in beams into the formulation of hydraulic fracture initiation/breakdown problems, then by replacing tensile strength σ_t in equation (6) with breakdown pressure P_b we have

$$p_b(t_1) = (1 - \chi(t_0, t_1)) \cdot p_b(t_0) \qquad (7)$$

We can rewrite this equation as

$$1 - \chi(t_0, t_1) = \frac{pressure\ required\ for\ breakdown\ after\ time\ t_1}{pressure\ required\ for\ \ breakdown\ after\ time\ t_0}$$

Or as

$$1 - \chi(t_0, t_1) = \frac{pressure\ required\ for\ delayed\ breakdown\ after\ time\ t_1}{pressure\ required\ for\ instantaneous\ breakdown}$$

where instantaneous breakdown occurs after a very short time, which in this study, we assume to be 1 second.

Kear and Bunger (2014) observed that applying a load of, say 90% of the material tensile strength, would cause failure at the same time, whether the rock was in 3 point bending, 4 point bending, or an indirect tension test. That is to say, the experimental evidence is that the measured value of χ is independent of the geometry used for testing it even though the nominal tensile strength does indeed depend on testing configuration.

This behavior was also observed in 3 and 4 point bending experiments performed by Lu et al (2015) using Coldspring Charcoal Granite, and these results suggest that χ is an intensive material property, dimensionless and independent of loading configuration.

2.6 FLUID PENETRATION β

After Hubbert and Willis (1957) and Haimson and Fairhust (1967) mathematically modelled the breakdown pressure and their predictions varied by a factor of two,

$$P_b = 3\sigma_h - \sigma_H + \sigma_t \quad \text{- Hubbert \& Willis}$$

$$P_b = \frac{1}{2}(3\sigma_h - \sigma_H + \sigma_t) \text{ - Haimson \& Fairhurst}$$

Detournay and Carbonell (1997) argued that neither prediction was wrong, but that they were for the extreme cases of no fluid penetration ('fast-pressurization') and full fluid penetration ('slow-pressurization') respectively.

Fluid penetration is the degree to which the fracturing fluid penetrates into the pores of the rock before breakdown occurs. The degree of fluid penetration is represented as dimensionless β and it has a range of $1 \leq \beta \leq 2$; where the lower value is for no fluid penetration and the higher value for full fluid penetration.

Haimson (1968) also noted from his experiments that when fluid penetrates into the rock, it increases the pore pressure of the rock and creates additional stresses that lower the breakdown pressure. This view was also espoused in experiments performed by Scott et al (1953) where drilling mud was used as the fracturing fluid in a pseudo no-penetration case.

The value of β was initially thought to be constant regardless of the duration of pressurization, but this may not be so. In delayed breakdown experiments using granite, an impermeable rock, Lu et al (2015) observed a steadily increasing deviation between predicted and experimental time to failure. The longer the time to initiation, the higher the deviation was. They proposed that the fractures initiated after long times had moved from the expected 'fast', 'non-penetrating',

'Hubbert &Willis' case to the 'slow', 'penetrating', 'Haimson & Fairhurst' case, and that even in an impermeable rock, some degree of fluid penetration – hence an increase in β – can occur when the time to failure is over hundreds of seconds. This increase in β leads to a larger than expected applied stress (following equation 1) and consequently, a shorter time to failure.

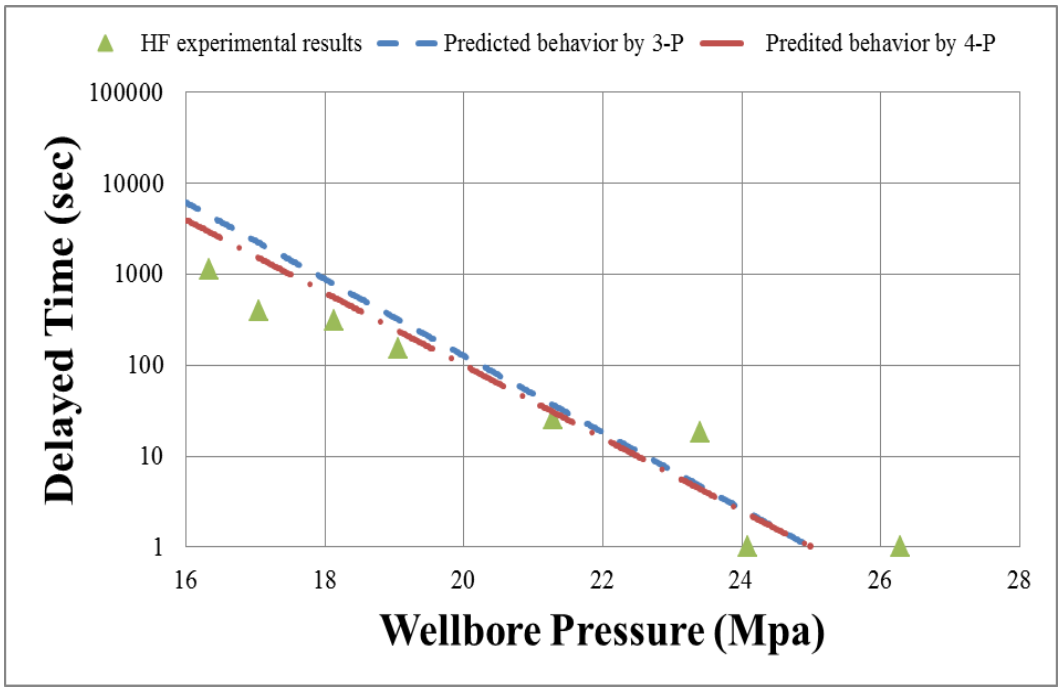

Figure 6: Experimental and Theoretical Comparison of Delayed Breakdown Pressures from Lu et al (2015). Notice the progressively lower-than-expected breakdown pressure from right to left.

2.7 STRESS ANISOTROPY RATIO

The state of stress underground involves two horizontal stresses that are rarely ever equal. The stress anisotropy ratio is a ratio of the smaller horizontal stress (σ_h) to the larger horizontal stress (σ_H). With limiting values of 0 and 1, a high stress anisotropy ratio implies a minimal difference

between the two stresses, hence a low degree of stress anisotropy. The stress anisotropy ratio in petroleum reservoirs is between 0.7-1.0.

2.8 POROELASTICITY, BIOT'S COEFFICIENT AND POISSON'S RATIO

Poroelasticity is the study of how fluid infiltration changes the mechanical behavior of a porous solid. Biot (1941, 1955, 1956) provided mathematical models to explain not only the fluid motion within the pores, but the structural displacement of the matrix. The Biot's coefficient is a measure of the ratio of the water volume squeezed out of the rock to the volume change of the rock if it is compressed while allowing the water to escape (Biot 1941). Typical values of the poroelastic coefficient for the Biot's coefficient is 0.6 for sandstone and 0.9-1 for shales.

For a material under axial deformation, Poisson's ratio is the ratio of lateral to longitudinal strain. Poisson's ratio is constant, dimensionless and an intrinsic property between 0 and 0.5. In rocks, the Poisson's ratio is typically between 0.15-0.35.

2.9 CONDITIONS THAT FAVOR DELAYED INITIATION OF ADDITIONAL FRACTURES

Bunger and Lu (2015) made theoretical predictions regarding the geological and petrophysical conditions that favor delayed initiation of hydraulic fractures – shallow reservoirs, low stress anisotropy ratio, small variation in rock tensile strength and in-situ stresses.

This work attempts to experimentally observe the role confining stresses and fluid penetration play in delayed initiation of hydraulic fractures. Understanding controlling parameters will help more accurately predict favorable conditions.

3.0 EXPERIMENTAL PROCEDURE

3.1 ROCK SELECTION

Agra Red sandstone and Coldspring Charcoal granite were chosen for the experiments. Sandstone because it provided similarity to hydrocarbon bearing rocks – porous, permeable, having fine grains as well as fairly visible bedding planes indicating a degree of intrinsic heterogeneity. Granite because it is a good example of an impermeable rock, has relatively high tensile strength and so can be tested under moderate to high confining stress.

3.2 SAMPLE PREPARATION

Pre-cut and polished sandstone and granite blocks measuring 6″ x 6″ x 6″ were purchased. A ½ ″ hole was drilled in each block using a diamond core bit, the hole drilled parallel to the bedding planes for the sandstone. The samples were then dried in ambient temperature of 21^0C for at least/ 72 hours to minimize the presence of moisture introduced by the drilling. This step was added to ensure the same initial conditions for each experiment and to maximize the bond strength of the epoxy used in the sealing of the analogue wellbore.

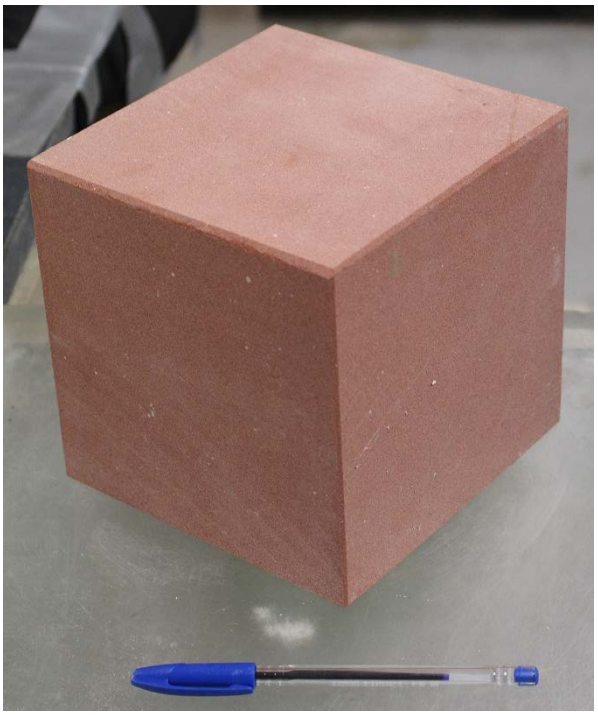

Figure 7: Agra Red Sandstone

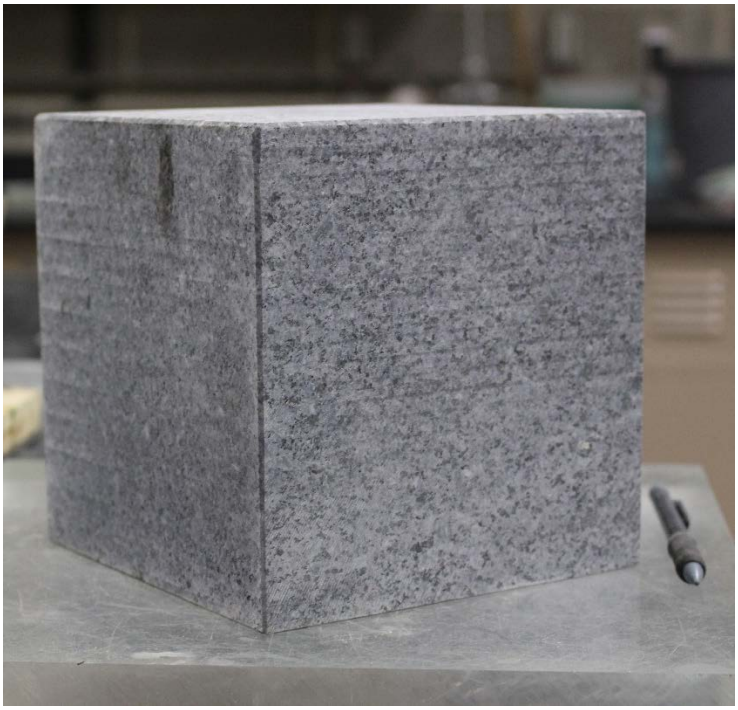

Figure 8: Charcoal Granite

3.2.1. No fluid penetration experiments

The first experiments test the end-member behavior with zero penetration. This is analogous to an infinite viscosity fluid and verifying the behavior is important for understanding basic mechanisms of wellbore breakage, jacketed treatments in the field are performed using inflatable packers for stress tests. To create hydraulic fractures in sandstone with zero fluid penetration, a ¼ ″ steel tube with perforations at its midriff was enclosed in a latex sheath having no mechanical properties that would impact the experiment. This sheath was tied at both ends using safety wire, before inserting into the rock. The sheathed part is 4” long.

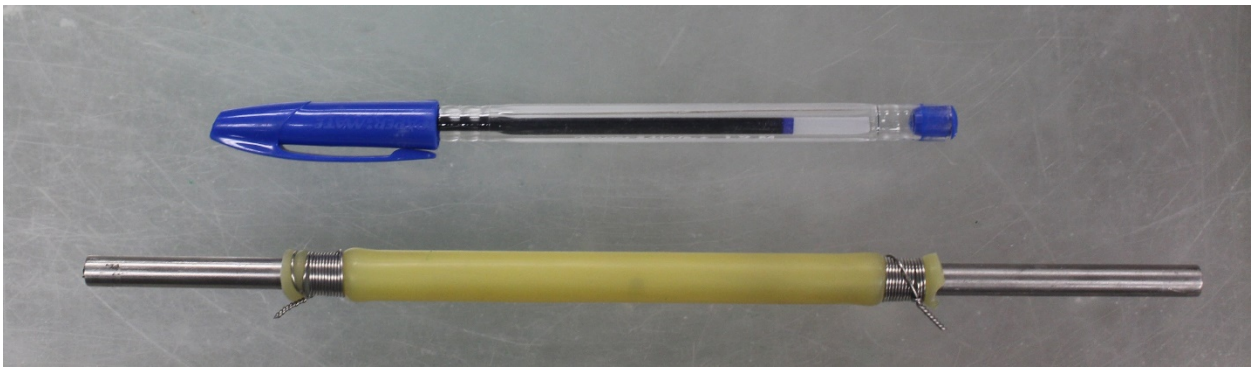

Figure 9 : The steel tube with the latex sheath tied over it

O-rings and Swagelok nuts and ferrules were fixed at both ends. An air gun (at 80-90 psi) was used to temporarily inflate the injection tube system. With a potting syringe and starting at the top hole, epoxy adhesive (Sikadur market brand) was injected to cover parts of the latex that were not in contact with the rock. This was to prevent the latex from bursting under pressure at these point. In initial experiments where this was not done or done poorly, at high pressures, the latex would fail at this area and fluid would leak-off into the rock. This failure would be audible and would show as a spike (sharp pressure decline and a gradual rise after) in the pressure record from the data acquisition system. This is further discussed in Section 4.7.

Two O-rings, both 0.5″ OD and 0.25 ″ ID were inserted just atop the Sikadur and then more Sikadur was used to fill the hole to surface. The O-rings prevent axial expansion of the latex sheath; limiting its expansion to the lateral direction. After 12 hours the block was carefully flipped over and the same procedure repeated on the other side. After another 12 hours the sample is removed from the air gun and the Sikadur is given another 24 hours to fully cure.

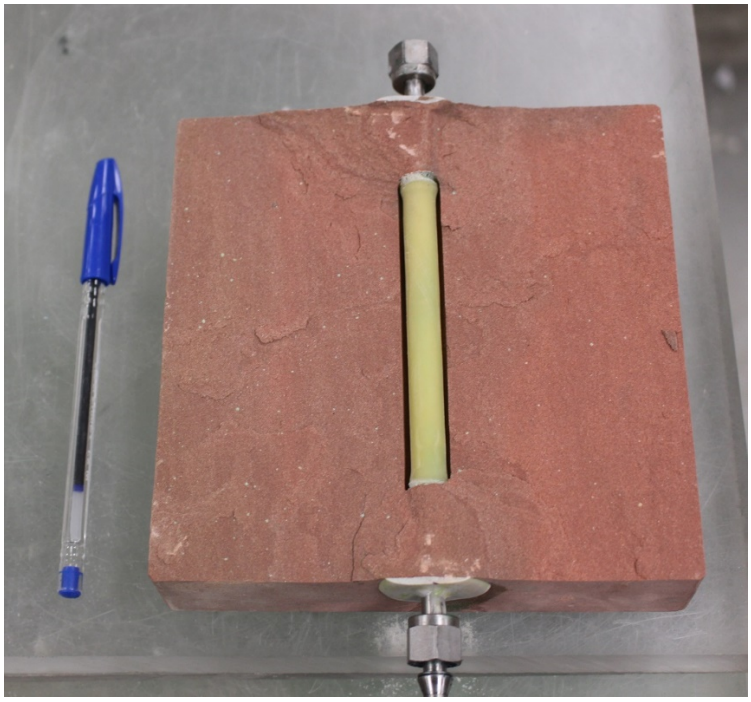

Figure 10: A view of the wellbore system in no-penetration experiment, after fracturing

3.2.2 Penetration (Full and Partial) Cases

For these experiments, a perforated $^{3}/_{8}$ ″ injection tube was used and O-rings (0.5″ OD and 0.375 ″ ID) inserted about $^{3}/_{4}$ inch deep at both ends. These O-rings are used to keep the fluid in the wellbore. Each side of the hole was filled with epoxy adhesive (Sikadur), one 12 hours after the

other. The block was then left for another 24 hours. This set-up was used in sandstone and granite.

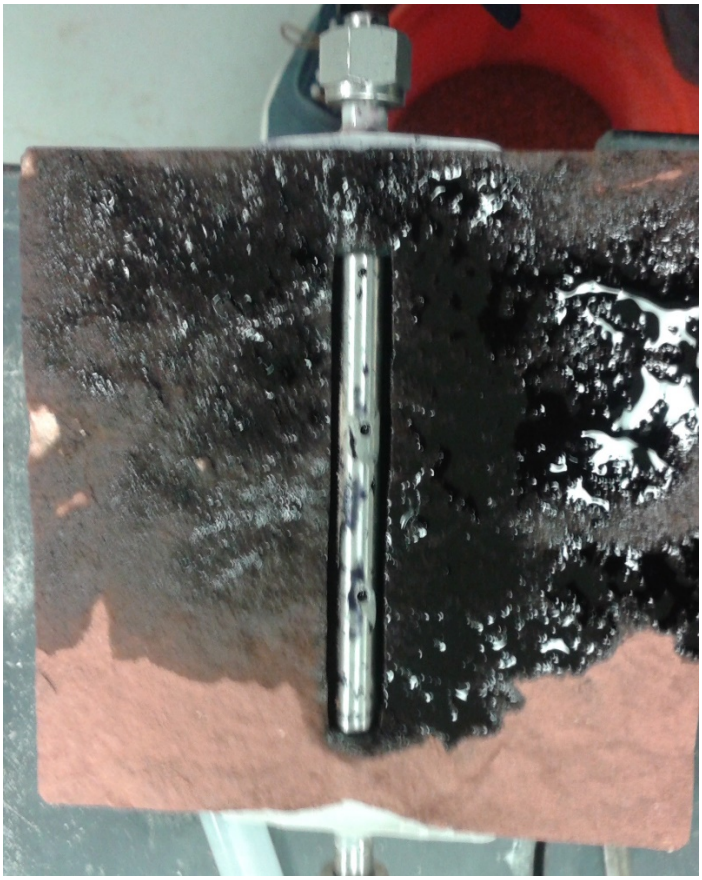

Figure 11: A view of a sandstone wellbore system in a penetration case, after fracturing with dyed glycerin

3.3 APPARATUS

3.3.1 Triaxial Stress Loading Frame

A custom built Enerpac RR-100-13 loading frame was used to apply vertical ‘overburden’ stress and four attached Nopak Class 3 series 3000 psi cylinders were used to apply the two horizontal stresses. This system used hand pumps for precise application and maintenance of the loading.

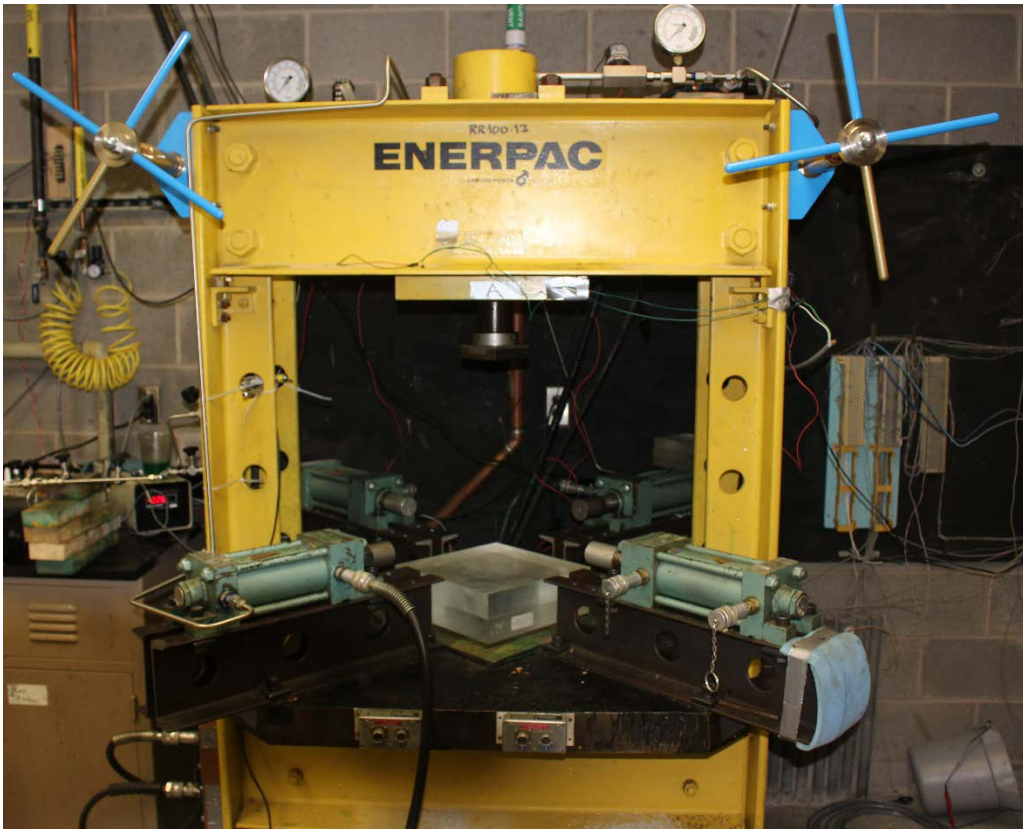

Figure 12: Triaxial Loading Frame

3.3.2 Wellbore Pressurization System

A 500D ISCO High Pressure Syringe Pump was used to generate wellbore pressure. The pump has an operating range of 10 – 3,750 psi.

Two custom built pressure interface vessels were used for fluids other than water (glycerin and vegetable oil). This vessel involves two connected pistons, each with a different area and fluid.

There is a transfer of energy between them and a pressure multiplication effect due to differing cross sectional areas of the pistons.

A Setra Pressure Transducer was used to measure pressure close to the wellbore for accuracy. The pressurization was connected to a WINDAQ Data Acquisition and Playback System that recorded pressure, time, flowrate and total flow.

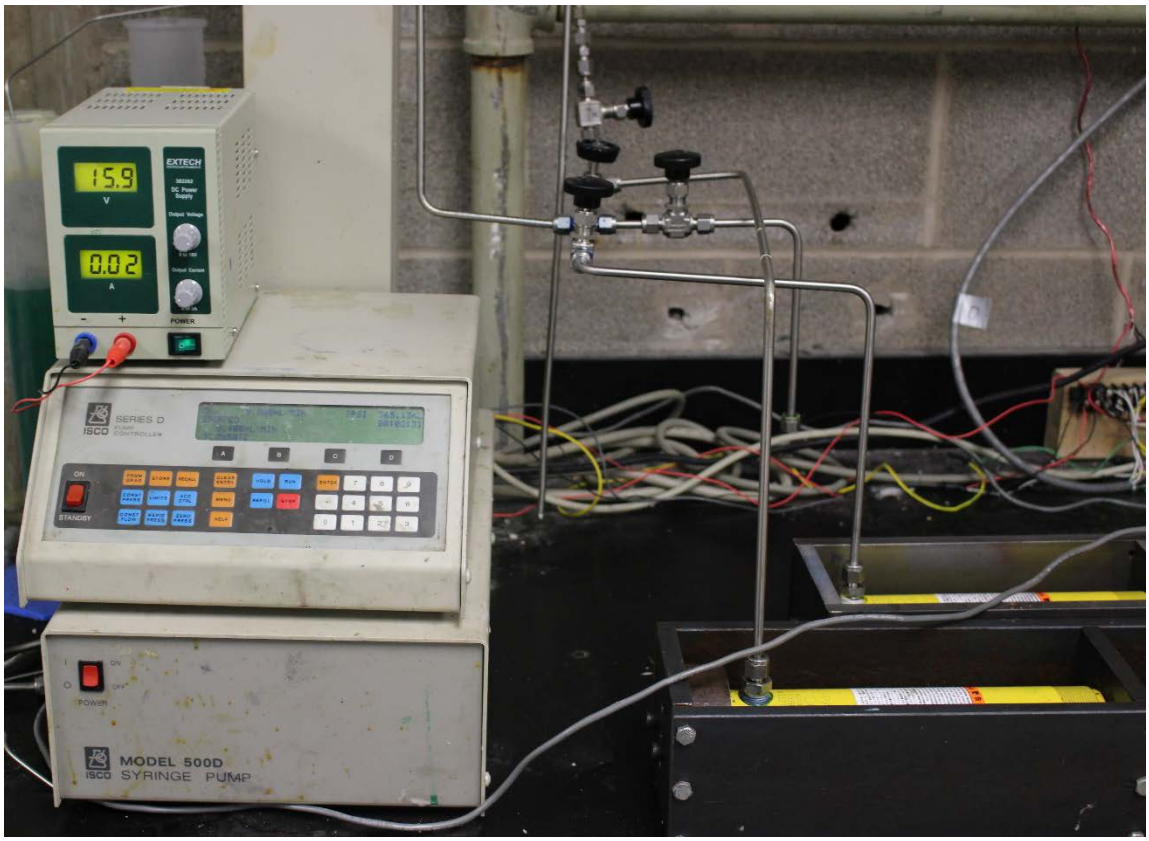

Figure 13: Wellbore Pressurization system: ISCO Pump and Pressure Interface Vessels

3.4 EXPERIMENTAL SET-UP AND PROCEDURE

3.4.1 Delayed Breakdown with No Confining Stress

The sample is connected to the pump using ¼ ″ steel pipe and the data acquisition system is begun. In the no fluid penetration experiments using the latex sheath, an initial pressure of 100 psi is given, so as to fill the piping and latex sheath with the fracturing fluid. This was not done with the penetration cases as the fluid would leakoff into the rock prior to the start of the experiment.

Afterwards the desired pressure is applied and data is recorded until after breakdown. The fracture is observed on the sample and observations recorded.

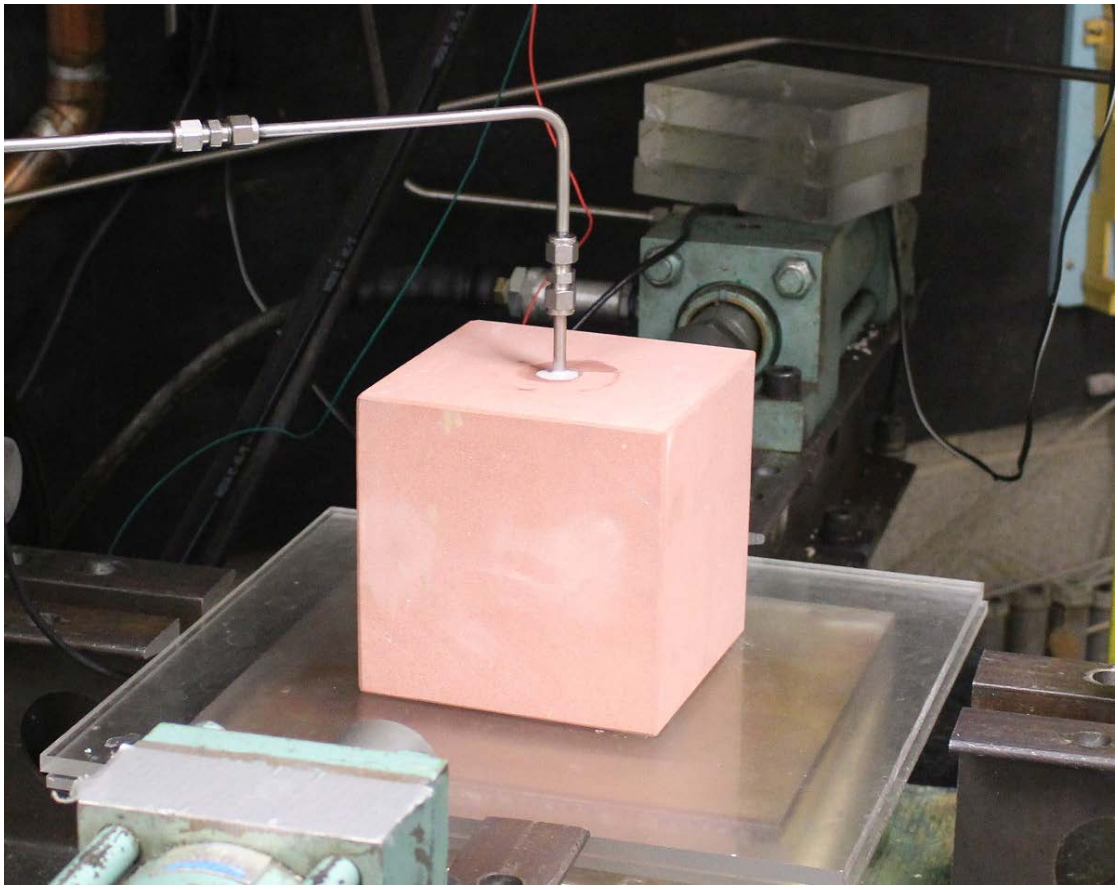

Figure 14: Delayed breakdown with zero confinement in sandstone

3.4.2 Delayed Breakdown with Confining Stress

Here, the sample is loaded into the frame and between 6″x1″x1″ acrylic sheets (as shown in Figure 15). The acrylic sheets help the external stress pistons not to exhaust their stroke length and they distribute the load from the piston evenly to the surface of the specimen.

After this, the pumps for the vertical and two horizontal stresses are run, one after the other until the desired amount of force is exerted. The applied stress should be slowly ramped up to desired level so as not to damage the material. Also when choosing the stress applied, the material's compressive strength should be taken into account.

When the external stresses are set, the data acquisition system is begun and the wellbore pressure, beginning with a 100 psi initial pressurization to fill up the latex sheath and piping where necessary, is applied. Data is recorded every half second until breakdown.

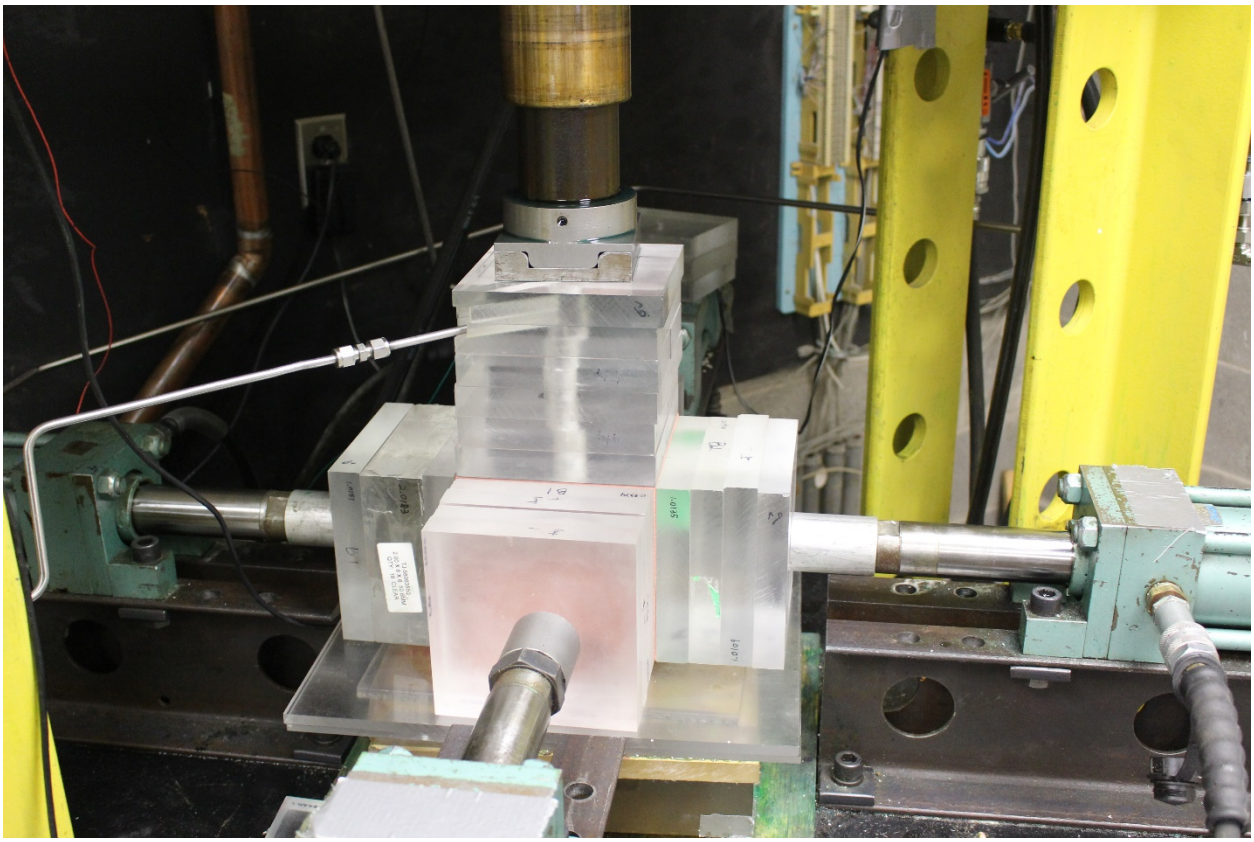

Figure 15: Delayed breakdown with confinement

3.4.3 Determination of Fluid Penetration Factor β for Different Fluids.

To determine penetration parameter (β) values, the procedure is the same as in 3.4.1, but here different fluids are used to fracture the sandstone blocks, and the instantaneous breakdown pressure recorded. The instantaneous breakdown pressure is gotten from pumping at a constant, moderate flowrate, and also by setting a high target pressure for the pump. This set point pressure, which is never attained but which ensures a high pressurization rate, should be about 1.5 to 2 times the expected breakdown pressure.

The selected cases are fractured with water, glycerin, vegetable oil, and a water-filled latex sheath. The interface vessel described in 3.3.2 was used in cases of oil and glycerin.
When water and glycerin are used as fracturing fluid, food-dye is added to enhance visibility.
To minimize the effect of rock heterogeneity, four set of experiments for each of the four cases were performed and an average value of the breakdown pressure calculated

4.0 RESULTS

4.1 MECHANICAL AND PETROPHYSICAL EVALUATION OF AGRA RED SANDSTONE

This data was provided by Coldspring USA who supplied the samples

Table 1: Mechanical properties of Agra Red sandstone

ASTM Test #	Test Name	Description	Value (N/mm2)	Value (PSI)
C-99	Modulus of Rupture	Dry - Parallel to Rift	12	1,740
C-99	Modulus of Rupture	Dry - Perpendicular to Rift	13	1,885
C-99	Modulus of Rupture	Wet - Parallel to Rift	7	1,015
C-99	Modulus of Rupture	Wet - Parallel to Rift	9	1,305
C-170	Compressive Strength	Dry - Parallel to Rift	93	13,489
C-170	Compressive Strength	Dry - Perpendicular to Rift	105	15,229
C-170	Compressive Strength	Wet - Parallel to Rift	56	8,122
C-170	Compressive Strength	Wet - Parallel to Rift	48	6,962
C97	Density		2.25 (S.G)	140 lbs/ft^3
C-97	Absorption	By Weight	3.95%	

The modulus of rupture test is the same as flexural or bending strength. It is used as an estimate of a material's tensile strength.

4.2 DETERMINATION OF β FOR DIFFERENT FLUIDS (NO CONFINING STRESS)

The results from evaluating the breakdown pressure, for the same rock but different fluids is shown below. Owing to rock heterogeneity and the dependence of breakdown pressure on flowrate, four runs were performed and an average value used.

Table 2: Breakdown pressures, β values and fluid viscosity.

Breakdown Pressure (P_b)	Glycerin	Water	Soybean Oil	Latex Sheath
Run 1 (psi)	1334	980	1373	2011
Run 2 (psi)	1550	839	1367	1618
Run 3 (psi)	1295	842	1370	1816
Run 4 (psi)	1587	839	1259	1636
Average P_b (psi)	1442	875	1342	1770
Is β known?	No	No	No	1.00
From equation 1 with zero confinement and zero pore pressure, $\sigma_t = \beta P_b$	N/A	N/A	N/A	1770
σ_t , the tensile strength, is a rock property and is constant therefore σ_t =	1770	1770	1770	1770
Use σ_t to find β since $\sigma_t = \beta P_b$	1.23	2.02	1.32	1.00

Notice the close correlation between ASTM C-99 estimate for tensile strength in Table 1 (dry & parallel to rift) and our tensile strength from breakdown pressure in Table 2 (also done dry and parallel to bedding).

4.3 DELAYED BREAKDOWN WITH NO CONFINEMENT AND NO FLUID PENETRATION (β=1)

Table 3: Delayed Breakdown experiments with no confinement and no fluid penetration

Test No	Pressure (psi)	Pressure (MPa)	Time to failure (sec)
1	1636	11.28	1.00
2	1400	9.65	5.60
3	1330	9.17	31.95
4	1178	8.12	98.65
5	1003	6.92	233.60
6	850	5.86	881.55
7	550	3.79	8619.00

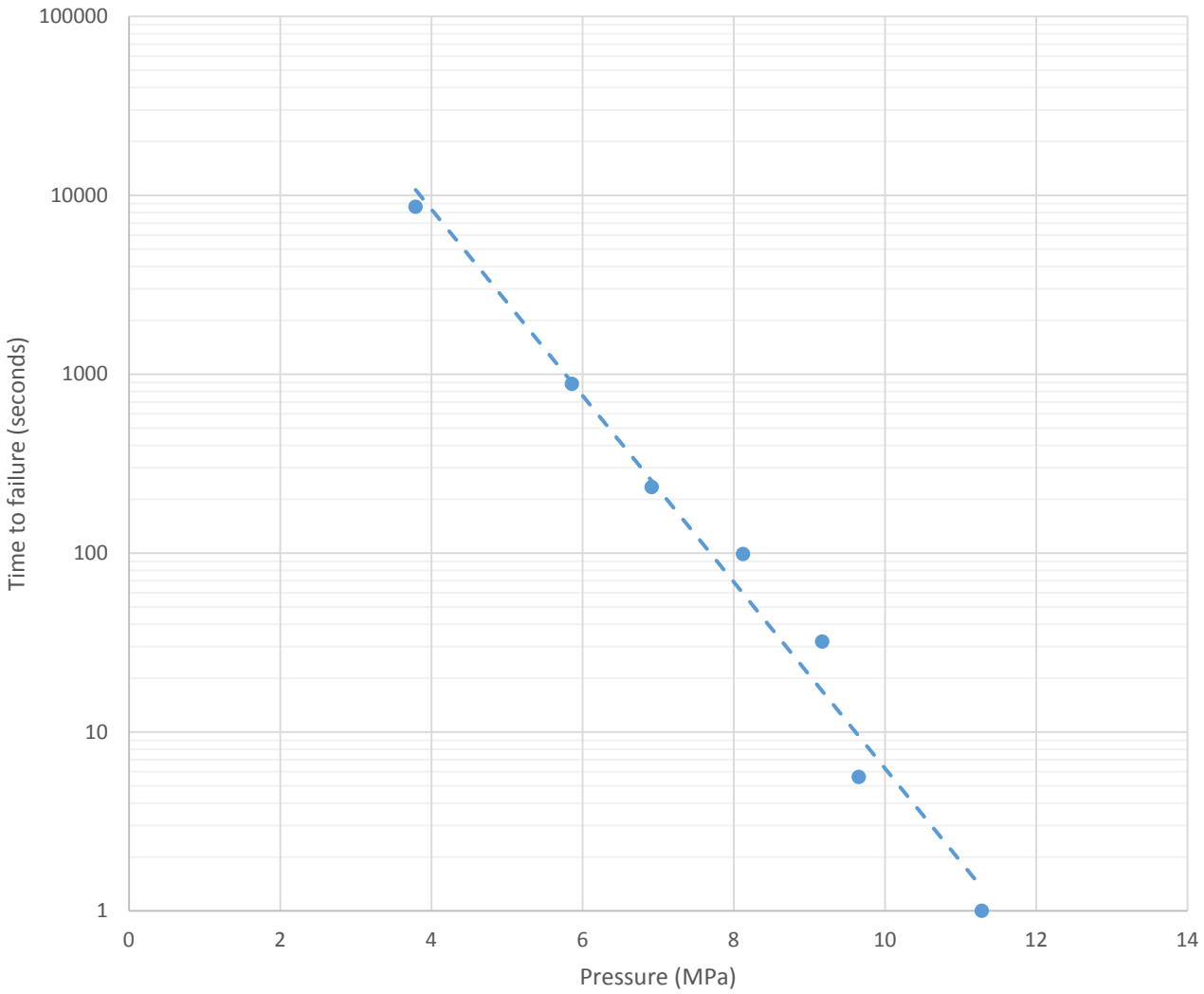

Figure 16: Time to failure vs Pressure curve for sandstone – no fluid penetration (latex jacketed) and no confinement.

4.4 DELAYED BREAKDOWN WITH NO-CONFINEMENT AND FULL FLUID PENETRATION (β =2)

Table 4: Delayed Breakdown experiments with no confinement and full fluid penetration

Test No	Pressure (psi)	Pressure (MPa)	Time to failure (sec)
1	450	3.10	150.00
2	840	5.79	1.00
3	550	3.79	307.00
4	395	2.72	505.10
5	605	4.17	29.10
6	660	4.55	15.25
7	691	4.76	20.05
8	361	2.49	935.2

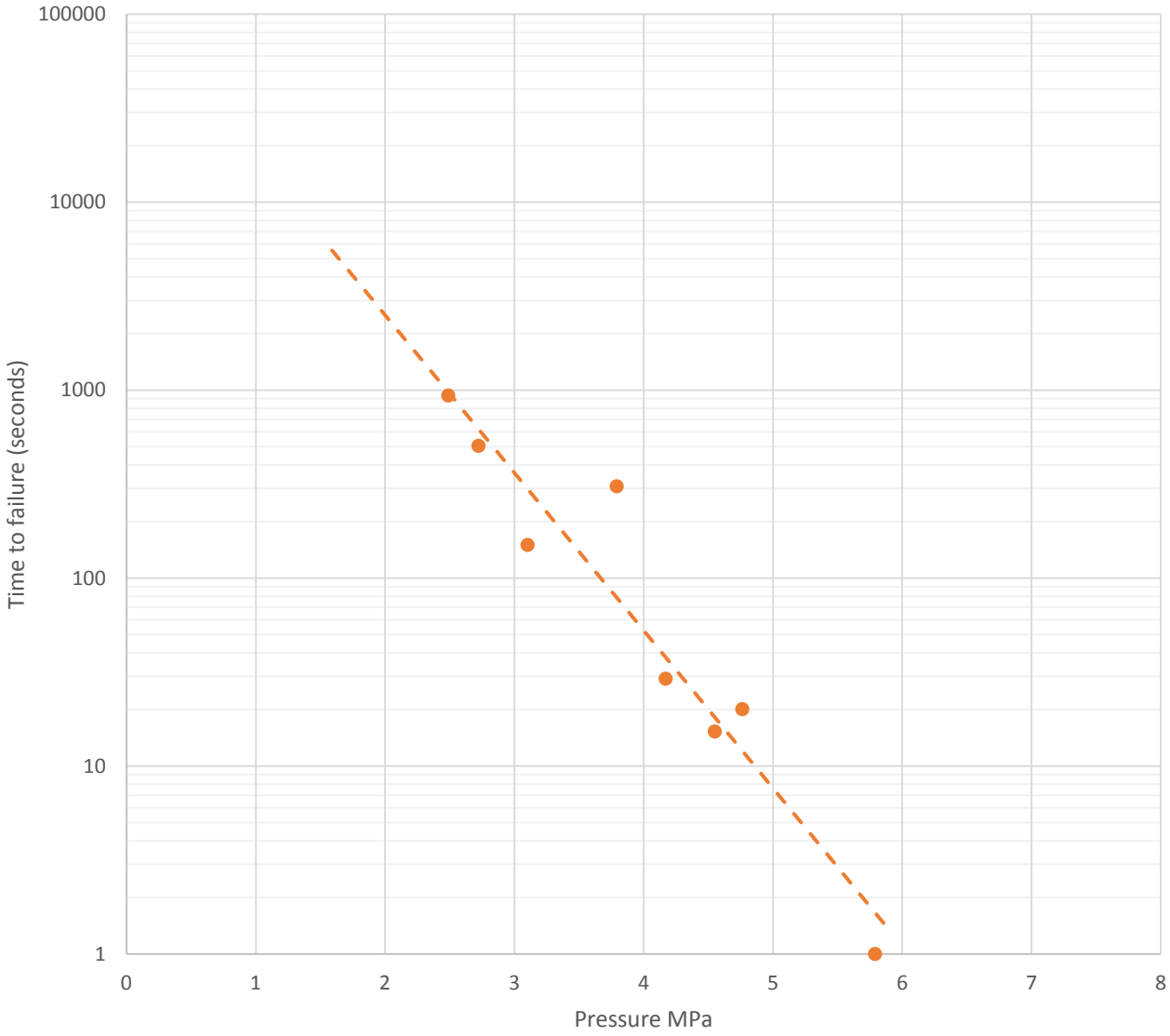

Figure 17: Time to failure vs Pressure curve for sandstone – full penetration and no confinement

4.5 VERIFICATION OF SET-UP USED FOR NO-FLUID PENETRATION CASES.

An important question is how do we know the latex sheath, in the no-penetration delayed breakdown experiments, was effective? After all, it eventually ruptures after the breakdown pressure is achieved. How is it confirmed it didn't rupture earlier? There are a number of evidences, described as follows.

4.5.1 Flowrate Difference

The fluid flowrate is a good indication of the efficacy of the latex sheath. Since water was used as the fracturing fluid, any leaks in the latex sheath would have caused the pump to supply additional fluid to maintain constant pressure. A look at the flowrate curves, one for both cases, at the same pressure (550psi) shows a marked difference in flowrate.

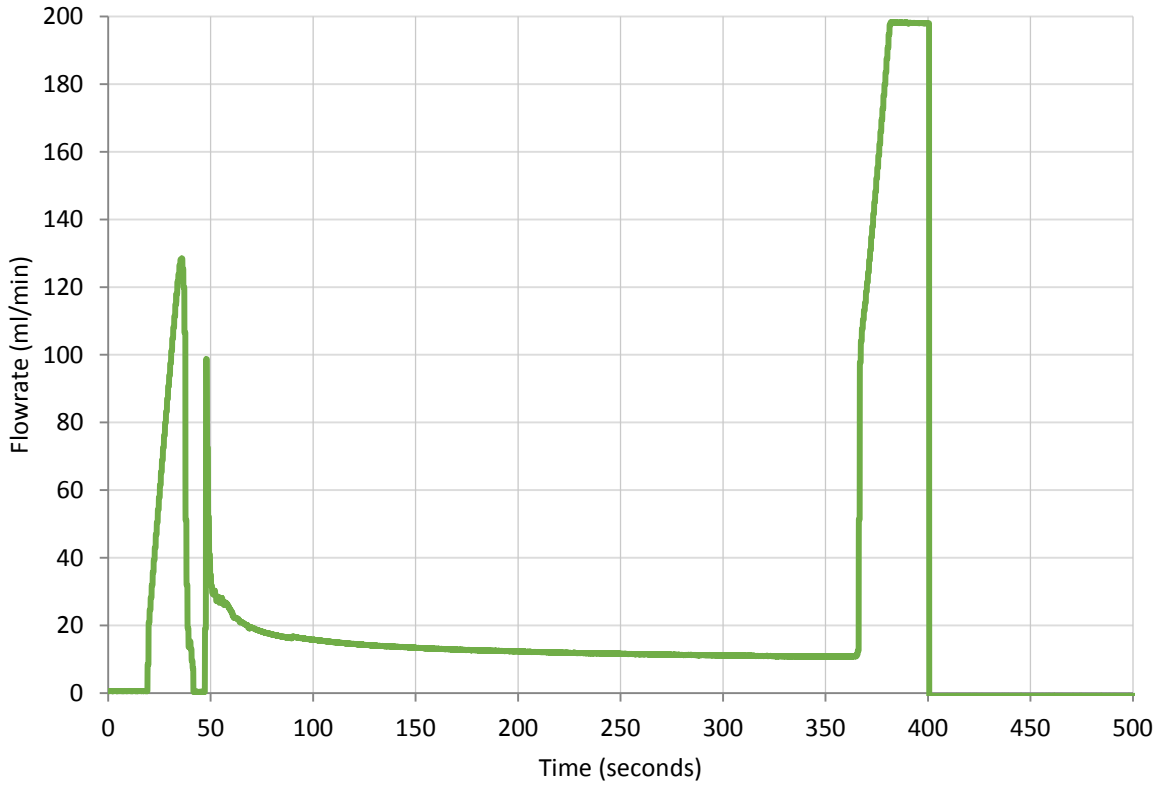

Figure 18: Flowrate for the full fluid penetration case

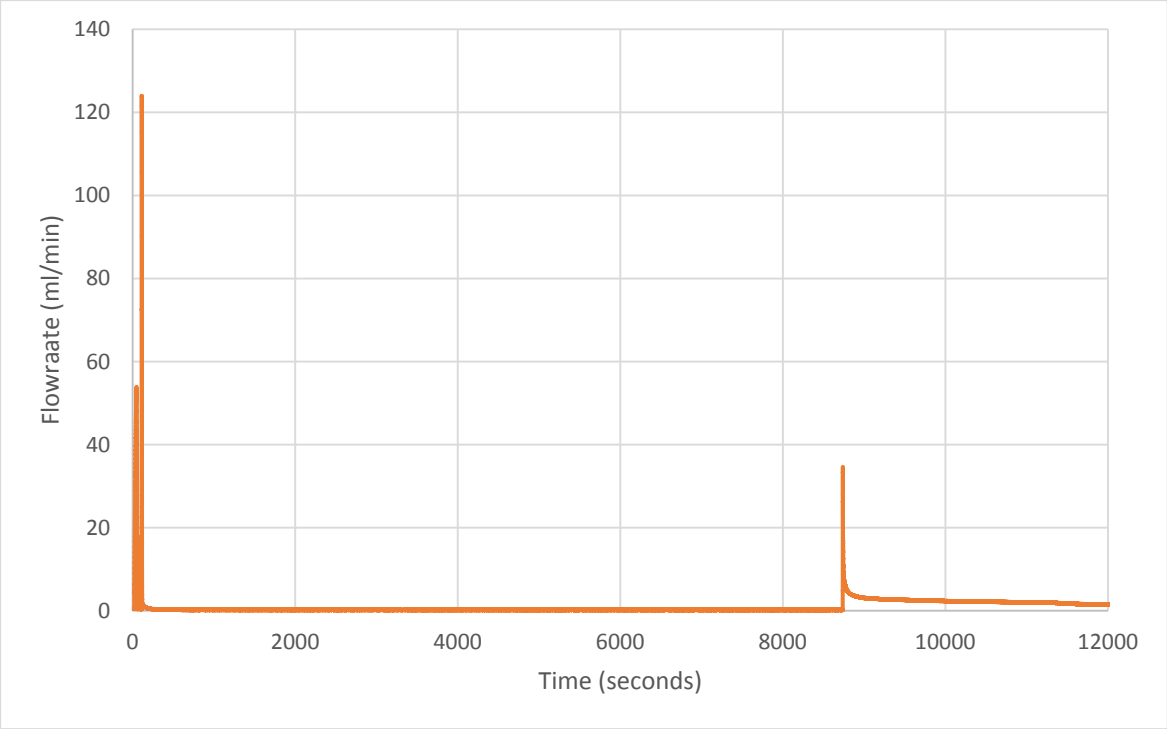

Figure 19: Flowrate for the no fluid penetration case

Notice during the constant pressure delay period for the fluid penetration case, the fluid flowrate is about 14 ml/min but for the no-penetration experiment using the latex sheath, the flowrate is 0.2 ml/min. The huge difference between the two is the additional fluid the pump has to supply to compensate for that which is continuously egressing into the pores of the rock, in the full fluid penetration case with water.

After the rock fails, and subsequently the latex sheath, the pump is still trying to hold the constant pressure, but there is a leak-off from a localized portion of the sheath, which shows up as an increase in flowrate, but still not as high as the un-sheathed experiment because the fluid penetration is localized i.e. the latex sheath bursts at one point and fluid leak-off into the rock occurs from that point.

4.5.2 Fluid Fingers

In fluid penetration experiments, before the fracture occurs , fluid leakoff into the rock becomes noticeable on the surface, but this is not the case for the no-penetration experiments as there is zero leakoff into the rock (fluid remains in the jacketed wellbore).

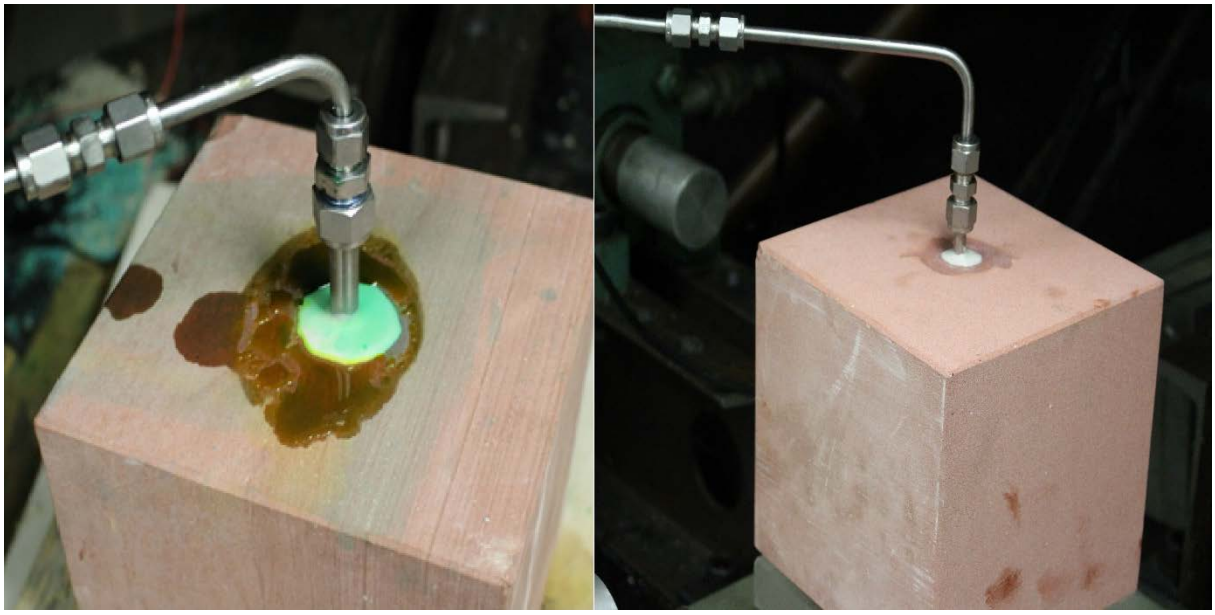

Figure 20: Fluid fingers, difference between fluid penetration ad no-penetration cases in sandstone. Green color in left image is from food dye added to water to enhance visibility.

4.5.3 Post-Fracture Analysis

To observe the wellbore after jacketed experiments, the pump is stopped immediately after the rock fractures, and just before the latex sheath fails. The rock is cut along the axis of the fracture and when fluid is pumped, it is possible to see the sheath still inflated. The area surrounding the wellbore is also dry. This is not so in unjacketed experiments.

Figure 21: Inflated latex sheath after no penetration fracturing experiment in sandstone. Green color inside inflated sheathe is from food dye added to water to enhance visibility.

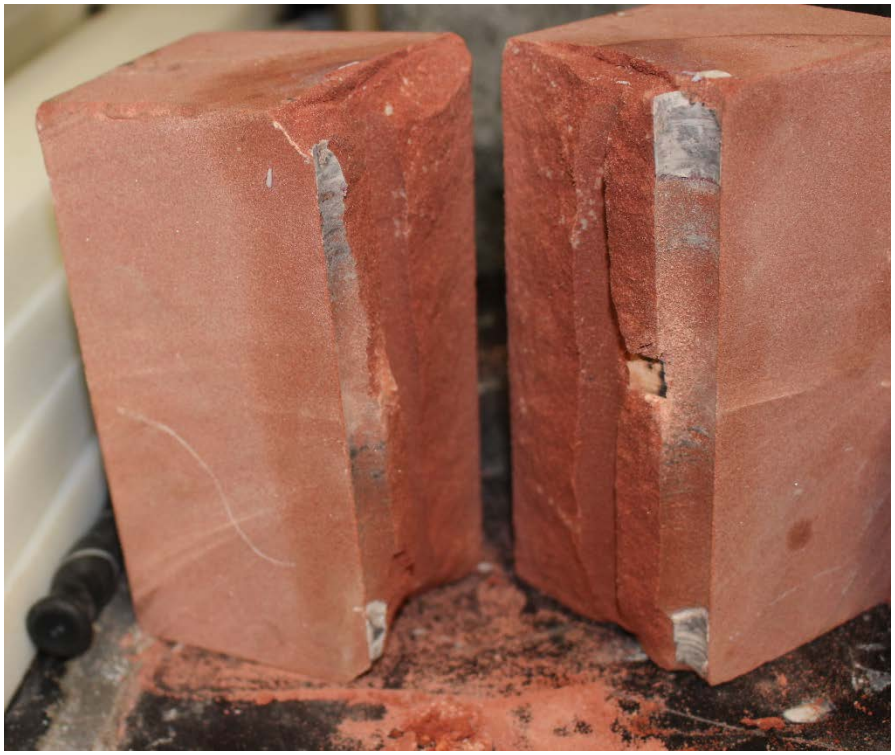

Figure 22: Wellbore after full penetration fracturing experiment in sandstone. Notice visible leakoff area.

4.5.4 Visible Fracture Dimensions

The fractures in cases of fluid penetration are fluid driven cracks, and from our observation, they appear to grow relatively larger than the no-penetration fractures which are not fluid driven.

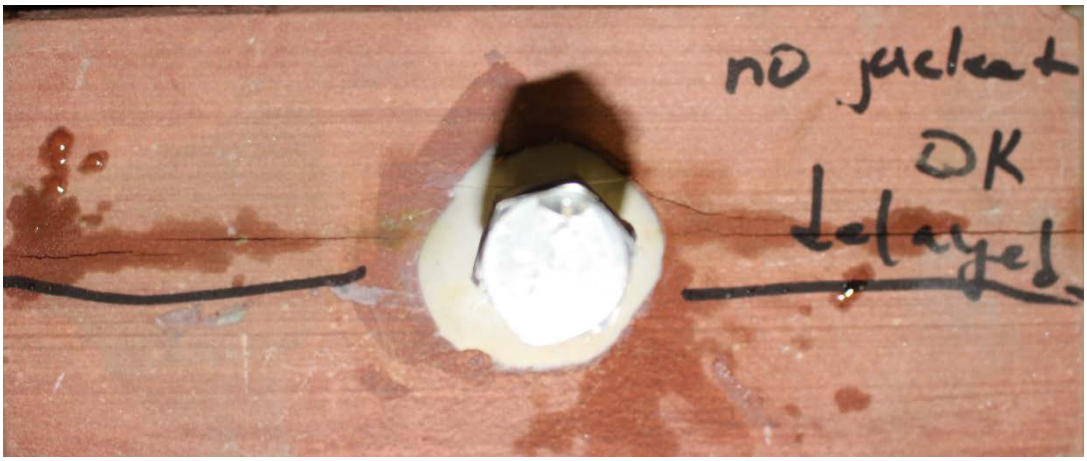

Figure 23: Visible fracture length and width in full penetration case with water in sandstone

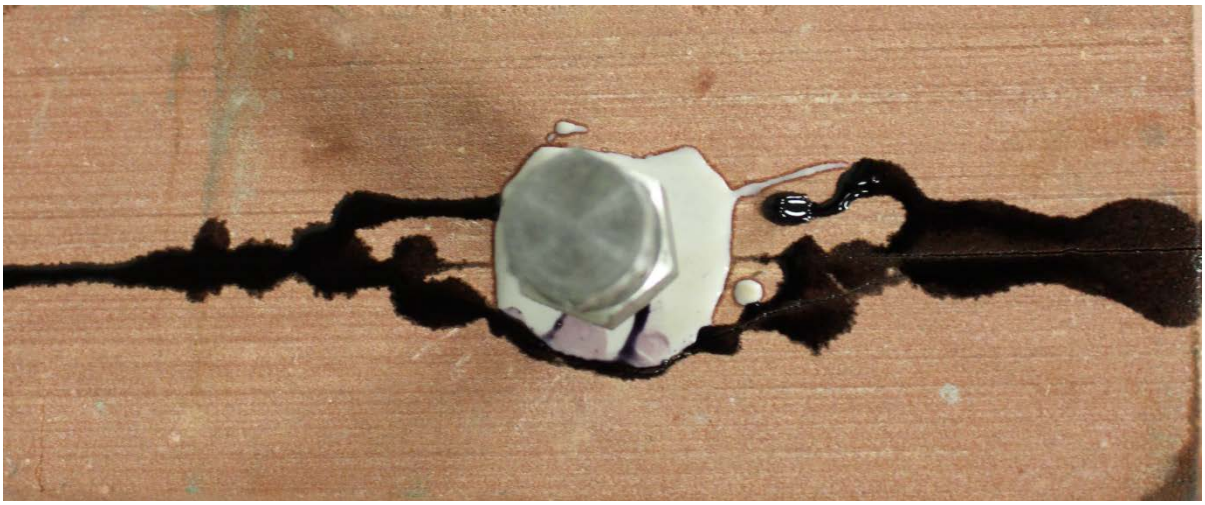

Figure 24: Visible fracture length and width in partial penetration case with glycerin in sandstone

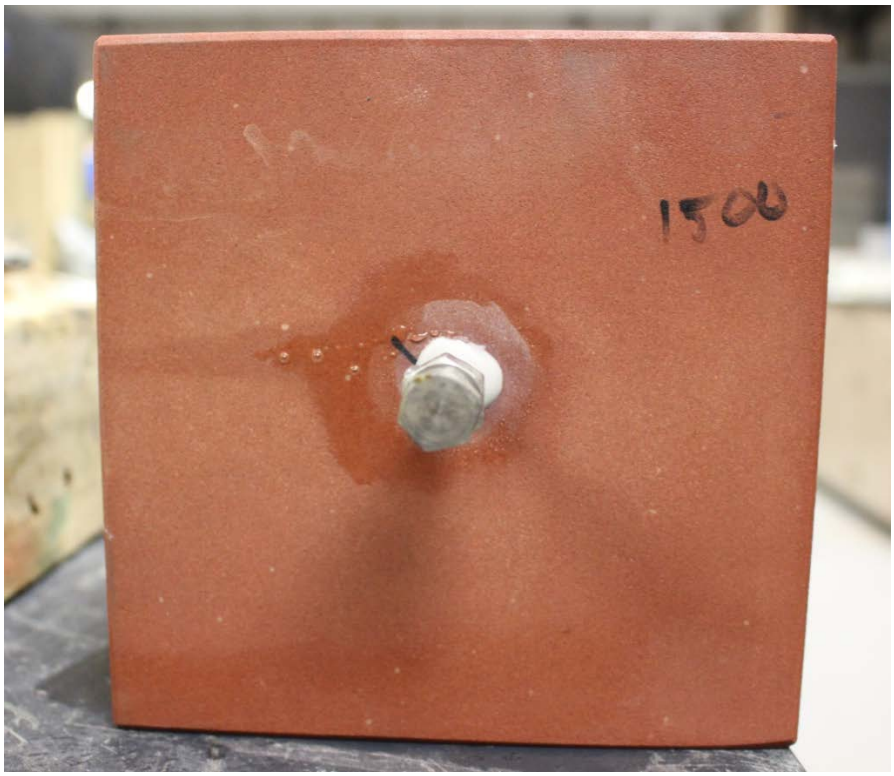

Figure 25: Very small fracture dimensions for the no-penetration case in sadstone. To observe the fracture, water has been splashed on the rock surface and 100psi air is pumped into the wellbore with an airgun, creating surface bubbles.

4.5.5 Pressure Record

In cases, where for reasons, such as an ineffectively-applied epoxy adhesive, the latex sheath fails before the rock fails, a noticeable sharp pressure decline and rise (a spike) is noticeable. The sharp drop is due to the sheath failure and subsequent expansion of fluid to fill the wellbore. The sound of the jacket bursting at high pressure is also audible.

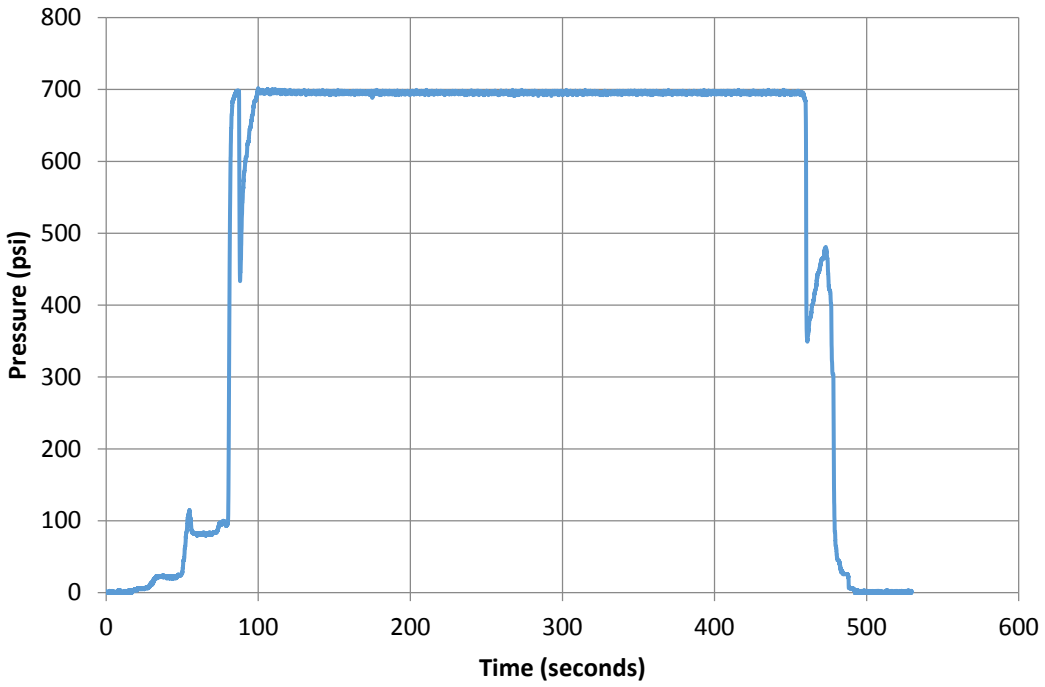

Figure 26: Pressure record from WINDAQ Data Acquisition system for an experiment where the latex sheath fails (indicated by the drop in pressure around 90 seconds) before the fracture initiates (indicated by pressure drop around 450 seconds).

4.6 DELAYED BREAKDOWN WITH LOW CONFINING STRESSES AND NO FLUID PENETRATION (β=1)

In this series of experiments confining stresses of σ_v, = 3.00 MPa, σ_H = 2.00 MPa and σ_h = 1.00 MPa were applied to the sample before wellbore pressurization.

Table 5: Delayed breakdown experiments in sandstone with low confinement and no fluid penetration

Test No	Pressure (psi)	Pressure (MPa)	Time to failure (sec)
1	2583	17.81	1.00
2	2320	16.00	42.80
3	1500	10.34	14900.00
4	1890	13.03	383.95
5	2016	13.90	350.50

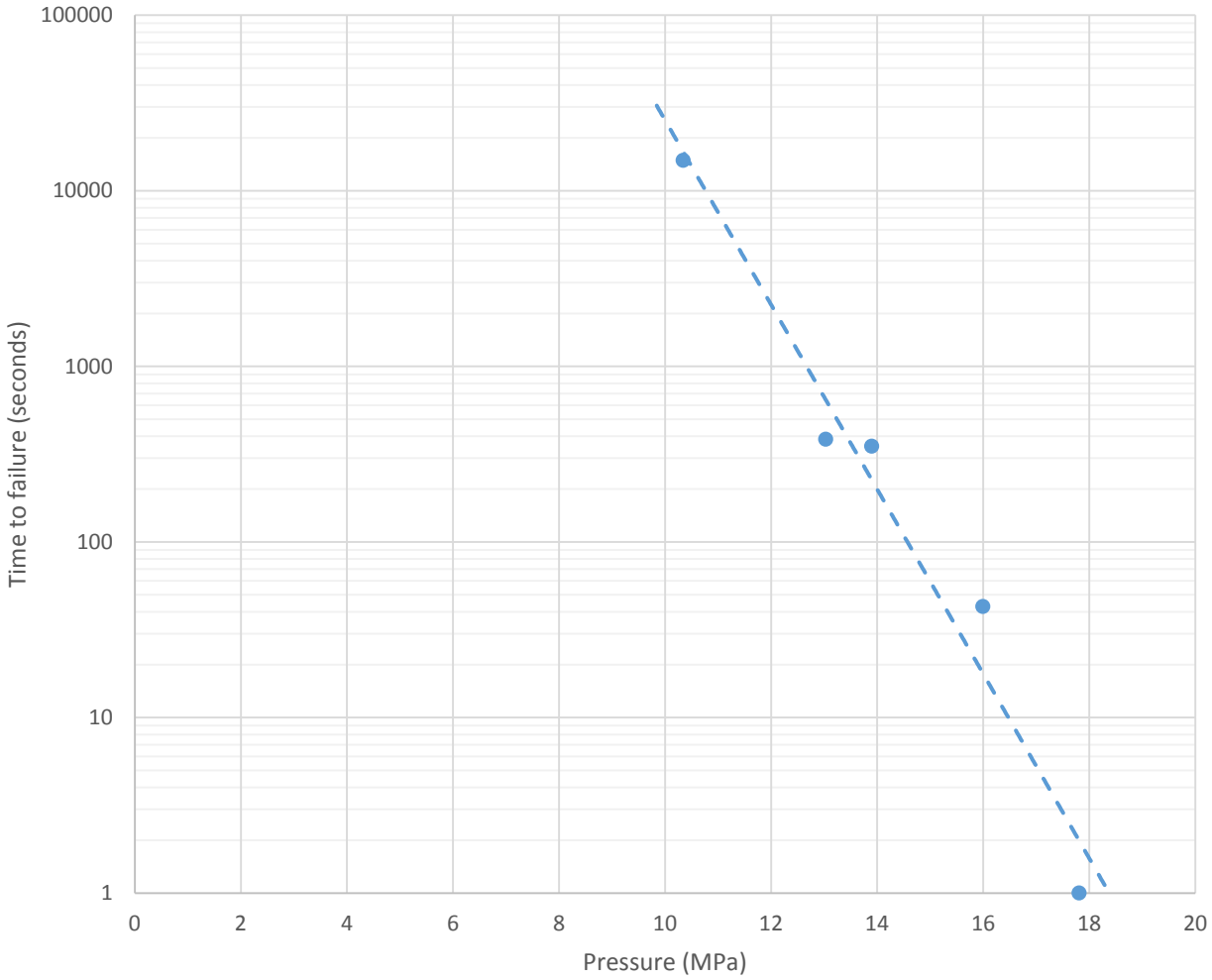

Figure 27: Pressure vs Time to failure for no penetration, low confinement case in sandstone.

4.7 DELAYED BREAKDOWN WITH LOW CONFINING STRESSES AND FULL FLUID PENETRATION (β=2)

Here we keep the confining stress same as in the no penetration case (σ_v, = 3.00 MPa, σ_H = 2.00 MPa and σ_h = 1.00 MPa) but here we allow full fluid penetration by removing the latex sheath and using water as fracturing fluid.

Table 6: Delayed breakdown experiments in sandstone with low confinement and full fluid penetration.

Test No	Pressure (psi)	Pressure (MPa)	Time to failure (sec)
1	1082	7.46	1.00
2	940	6.48	4.75
3	910	6.27	15.20
4	805	5.55	188.80
5	704	4.85	330.25
6	612	4.22	2587.35

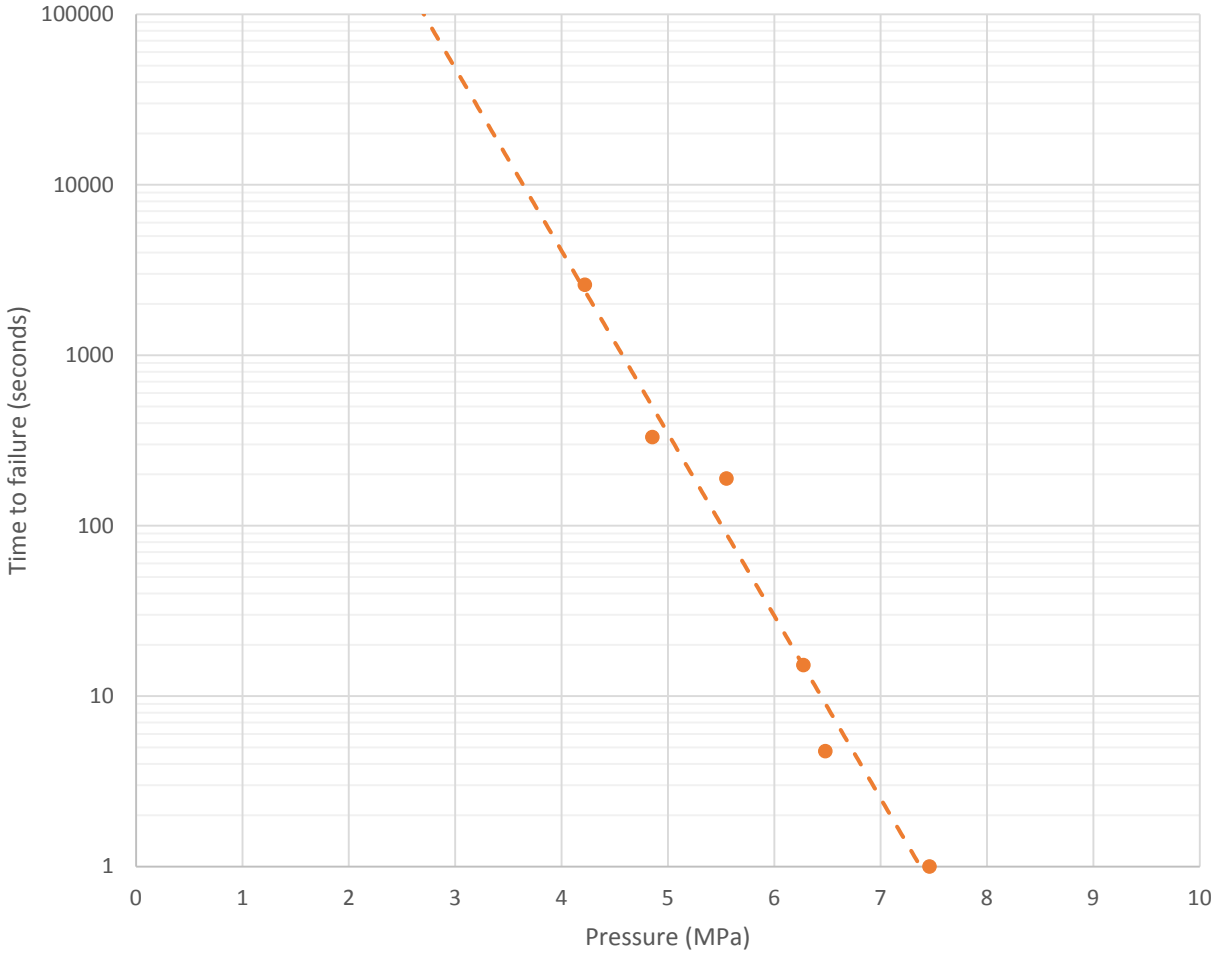

Figure 28: Pressure vs Time to failure for full penetration low confinement case in sandstone.

4.8 DELAYED BREAKDOWN WITH NO CONFINING STRESSES AND PARTIAL FLUID PENETRATION

It is also useful to demonstrate whether the theory is valid for the behavior of other rock. To this end, the same tests were carried out in charcoal granite. Apart from the fact that granite is geologically very different from sandstone, it is a material that can withstand high confining stress. When moderate to high stresses were applied on sandstone, it caused failure of the rock around the wellbore. The fracturing fluid used is this set of experiments is water.

First we perform these test without confining stress in charcoal granite

Table 7 : Delayed breakdown experiments in charcoal granite with no confinement.

Test No	Pressure (psi)	Pressure (MPa)	Time to failure (sec)
1	1680	11.58	163.90
2	1793	12.36	81.50
3	1582	10.91	3079.15
4	1920	13.24	13.80
5	1955	13.48	4.30
6	2003	13.81	1.00

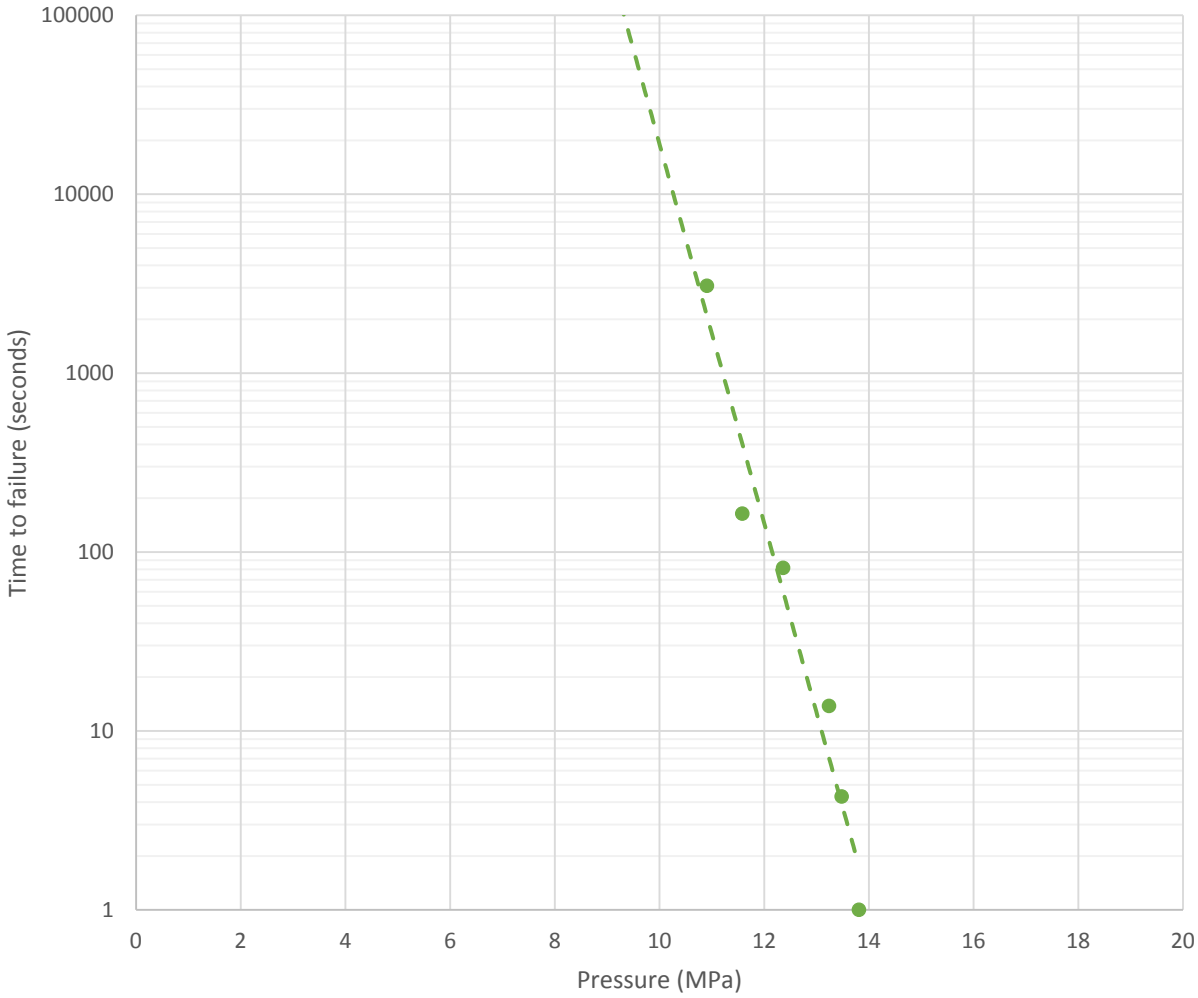

Figure 29 : Delayed breakdown experiments in charcoal granite with no confinement.

4.9 DELAYED BREAKDOWN WITH HIGH CONFINING STRESSES AND PARTIAL PENETRATION.

Here, charcoal granite were used, and the confining stresses of σ_v, = 7.08 MPa, σ_H = 4.77 MPa and σ_h = 3.33 MPa) were applied – highest first and lowest last – before wellbore pressurization and eventual breakdown. The stresses were such that available equipment could provide, and material integrity was possibly not compromised. The results are as shown in Table 8 below.

Table 8: Delayed breakdown experiments in charcoal granite with confinement.

Test No	Pressure (psi)	Pressure (MPa)	Time to failure (sec)
1	2663	18.36	1.00
2	2662	18.35	1.00
3	2300	15.86	2.50
4	2250	15.51	7.60
5	2200	15.17	18.00
6	2150	14.82	48.85
7	2117	14.60	105.00
8	2051	14.14	6006.50
9	2034	14.02	10510.00

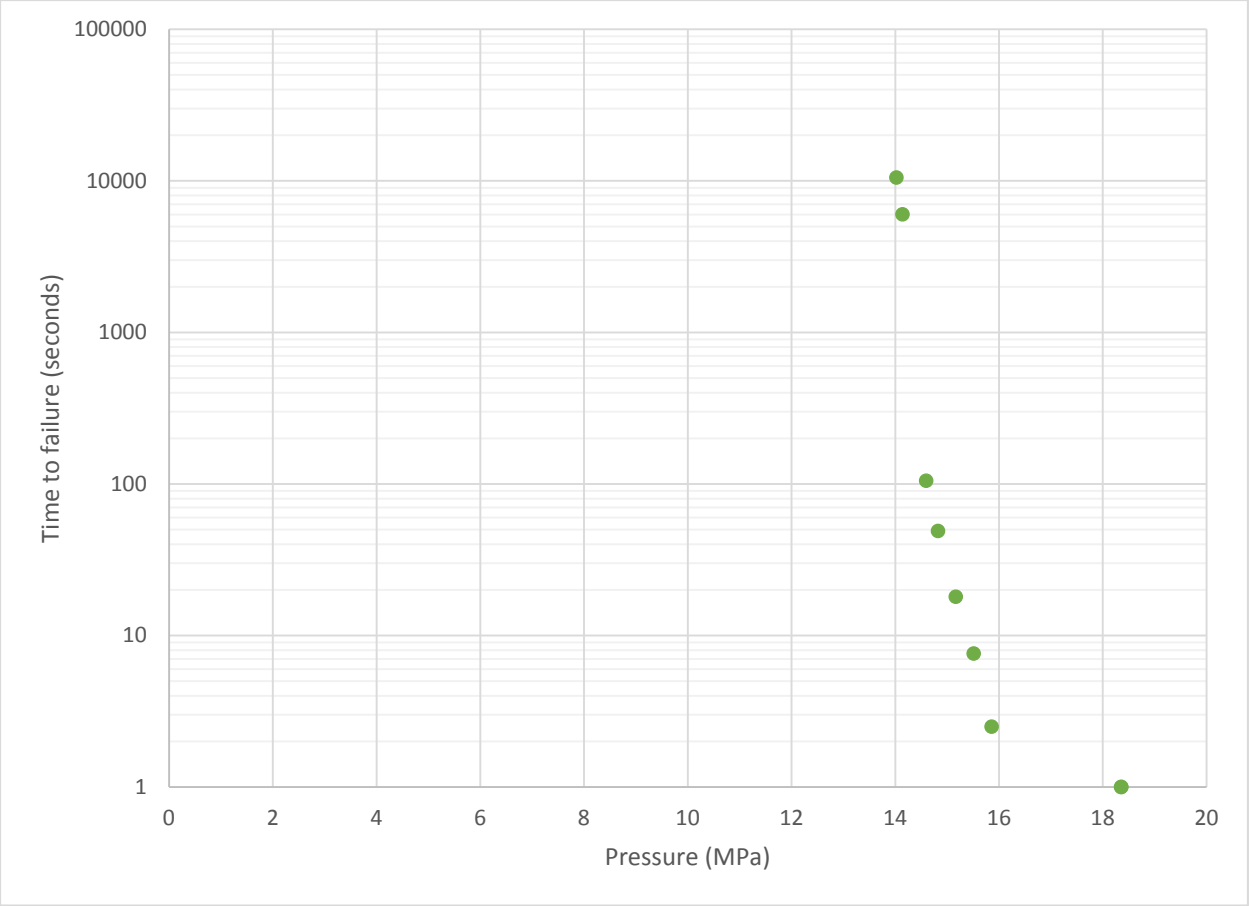

Figure 30: Delayed breakdown experiments in charcoal granite with zero confinement.

NOTE: In all cases we have assumed 1 second to be the time for instantaneous breakdown of the rock.

5.0 THE ROLE OF FLUID PENETRATION IN TIME-DEPENDENT INITIATION OF HYDRAULIC FRACTURES.

As indicated by Haimson (1968), fluid penetration elevates the pore pressure near the wellbore and comprises and additional contributor to fracture initiation. Hence a highly penetrating fluid will create hydraulic fractures at a much lower pressure than a non- penetrating fluid. Similarly, if a highly permeable rock and an impermeable rock have similar tensile strength, when fracturing with a penetrating fluid, breakdown will occur first in the permeable rock.

After Haimson (1968), the instantaneous breakdown pressure in the no fluid penetration and no confinement case can be used as a useful estimate of the tensile strength (this value also closely aligns with the ASTM C-99 tensile strength in Table 4.2).

Comparing this value with the full penetration case experiments using water, we observe that we can create a fracture after a delayed time of ~500 seconds at a pressure of 395psi (~25% of the tensile strength).

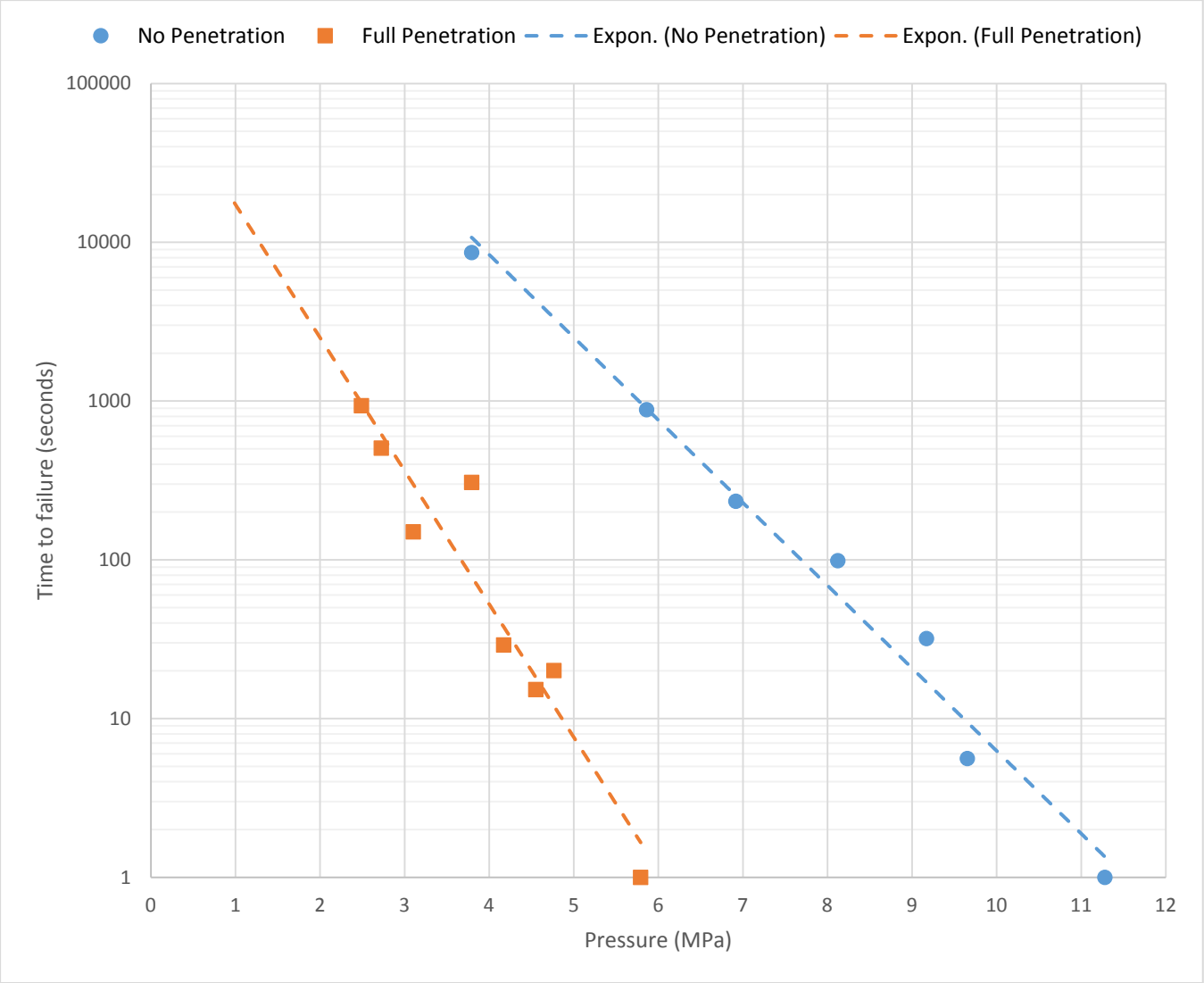

Figure 31: Curves for full penetration and no penetration delayed initiation in sandstone both with no confinement

A comparison of the two cases, full penetration and no penetration shows a shift of the curve to the right by a factor of two, as expected from theory.

If we use equation 5a to interpret the results, we see that the two curves, i.e. $\beta = 1$ (a no-penetration case) and $\beta = 2$ (a full penetration case), converge at $\sigma = 0$ *and* $t = A$. The magnitude of the divergence between them is always equal to β.

We also observe that moving from β=1 (a no-penetration case) to β=2 (a full penetration case), does not change the propensity of time-dependent fractures to initiate but only changes the relationship between time and pressure by a factor of β.

Table 9 : Comparison of no and full penetration cases both with no confinement in sandstone

Time (sec)	Full Penetration Case Pressure (MPa)	No Penetration Case Pressure (MPa)	Ratio (β)
10,000	1.3	3.7	2.84
1,000	2.5	5.7	2.28
100	3.8	7.7	2.02
10	4.8	9.6	2.00
1	6.0	11.4	1.90

The data is Figure 30 and Table 9 are for the case of zero confining stresses.

In the presence of the same confining stresses – and we discuss the impact of confinement in Chapter 6 – we can also evaluate if this relationship is the same.

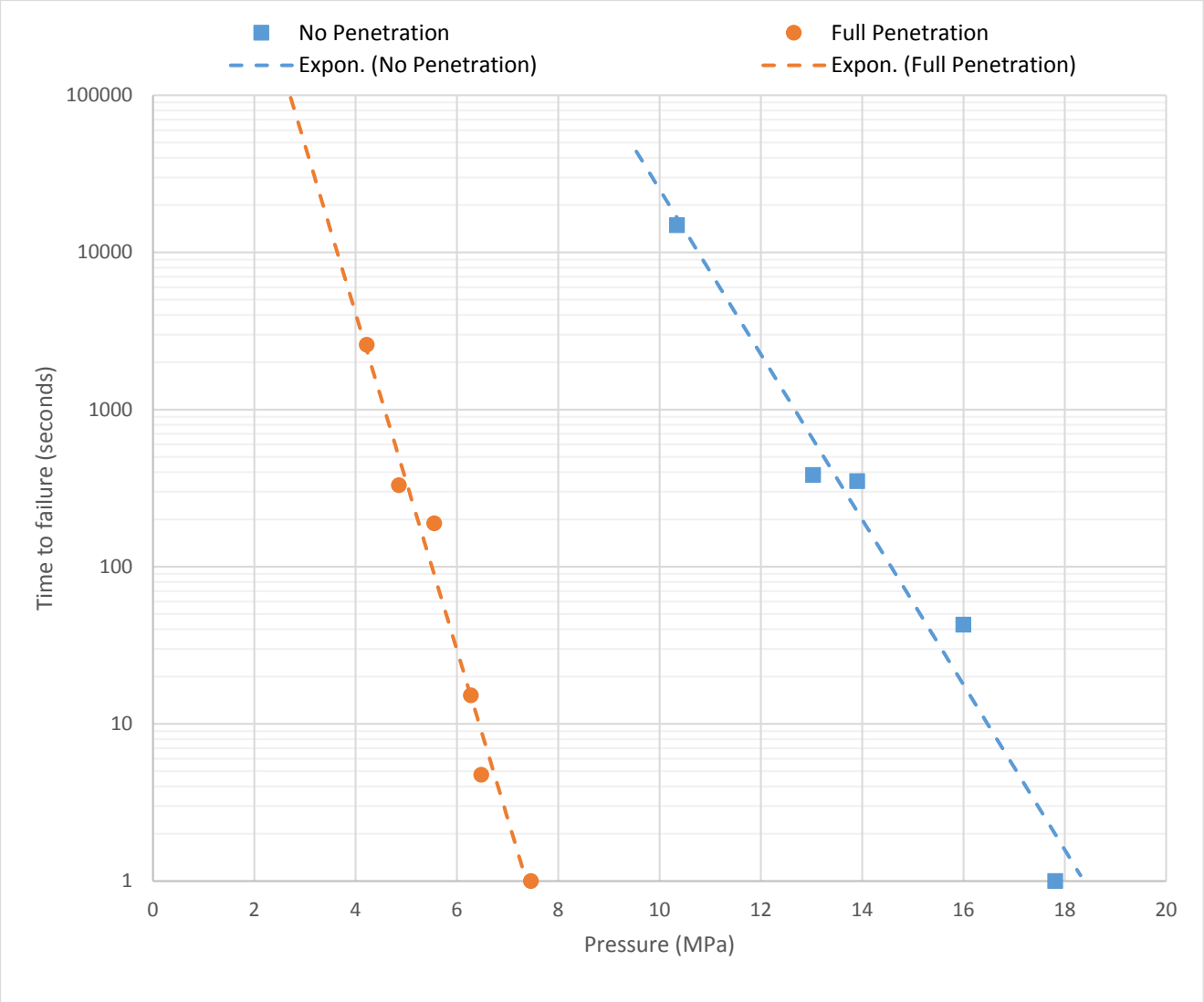

Figure 32: Curves for full penetration and no penetration delayed initiation in sandstone both with confining stresses. σ_v, σ_H and σ_h were the same in both set of experiments

Table 10: Comparison of no and full penetration cases both with confining stresses in sandstone

Time (sec)	Full Penetration Case Pressure (MPa)	No Penetration Case Pressure (MPa)	Ratio (β)
10,000	3.8	10.6	2.79
1,000	4.8	12.8	2.66
100	5.7	14.4	2.52
10	6.4	16.3	2.54
1	7.5	18.2	2.43

Recall equations 5b and 5d, restated below.

$$t = A * \exp[(-\gamma) * \sigma_{\theta\theta}^{(max)}/kT] \qquad (5b)$$

$$t = A * \exp[(-\gamma) * (\beta P_w - \hat{\sigma})/kT] \quad (5d)$$

If we plot, in the cases of confinement and no confinement, curves of time versus the applied tangential stress (the applied tangential stress $\sigma_{\theta\theta}^{(max)} = \beta P_w - \hat{\sigma}$) we expect the curves for full penetration and zero penetration to overlap (i.e. the applied stress should be the same, whether we are in the 'fast/no penetration' regime or 'slow/penetrating' regime.

Figure 32 shows the case for zero confining stress. We observe that the applied stress is approximately equal in both 'fast' and 'slow' cases. However, they are not equal in the case of confining stress. This anomaly serves as a harbinger to the discussion in Chapter 6 about the role of confining stresses in delayed initiation of hydraulic fractures.

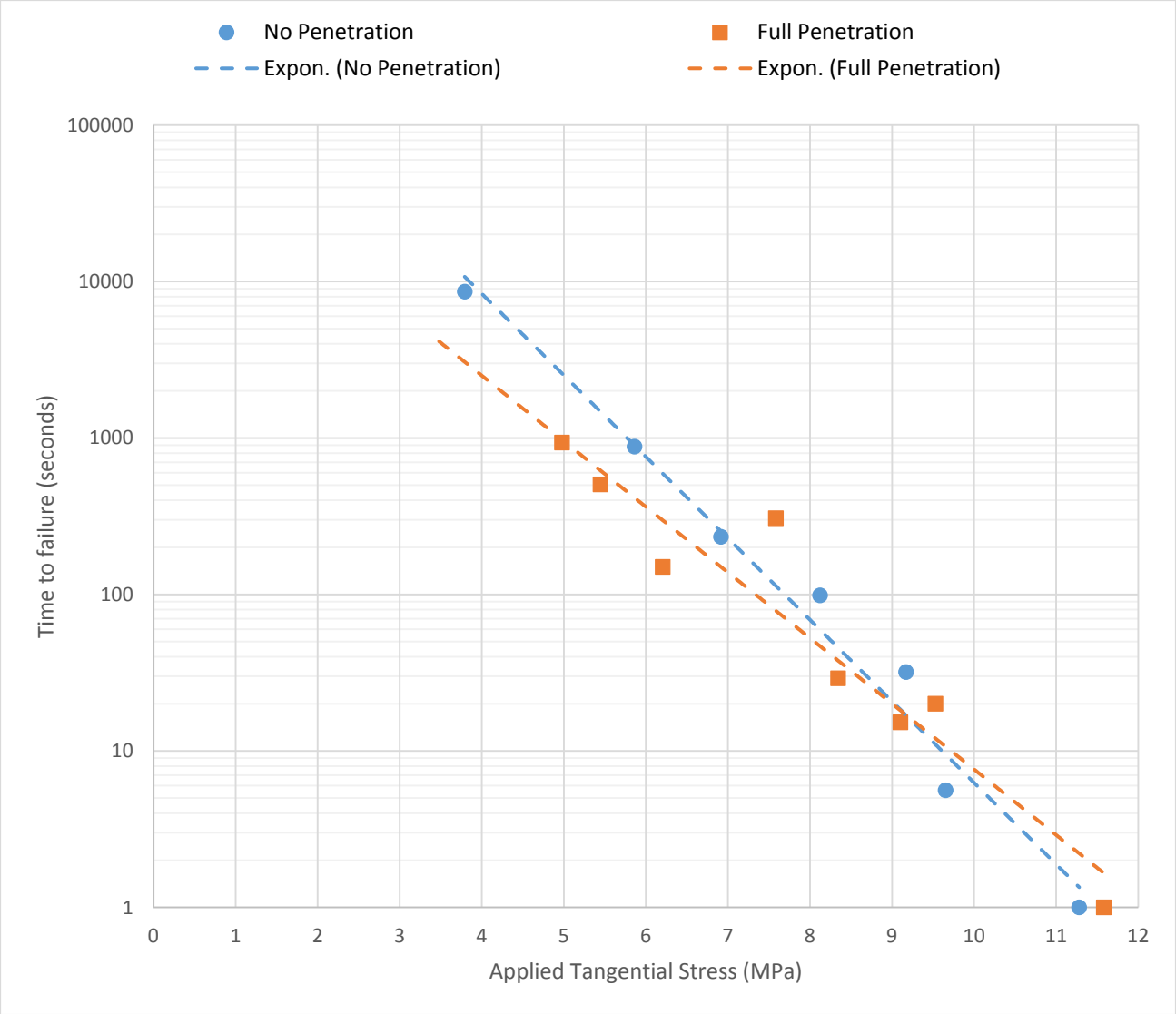

Figure 33: Comparison of the applied tangential stress for 'slow/penetrating' and 'fast/no penetration' cases with no confining stress in sandstone. Theory predicts both value to be equal and experimental values closely agree.

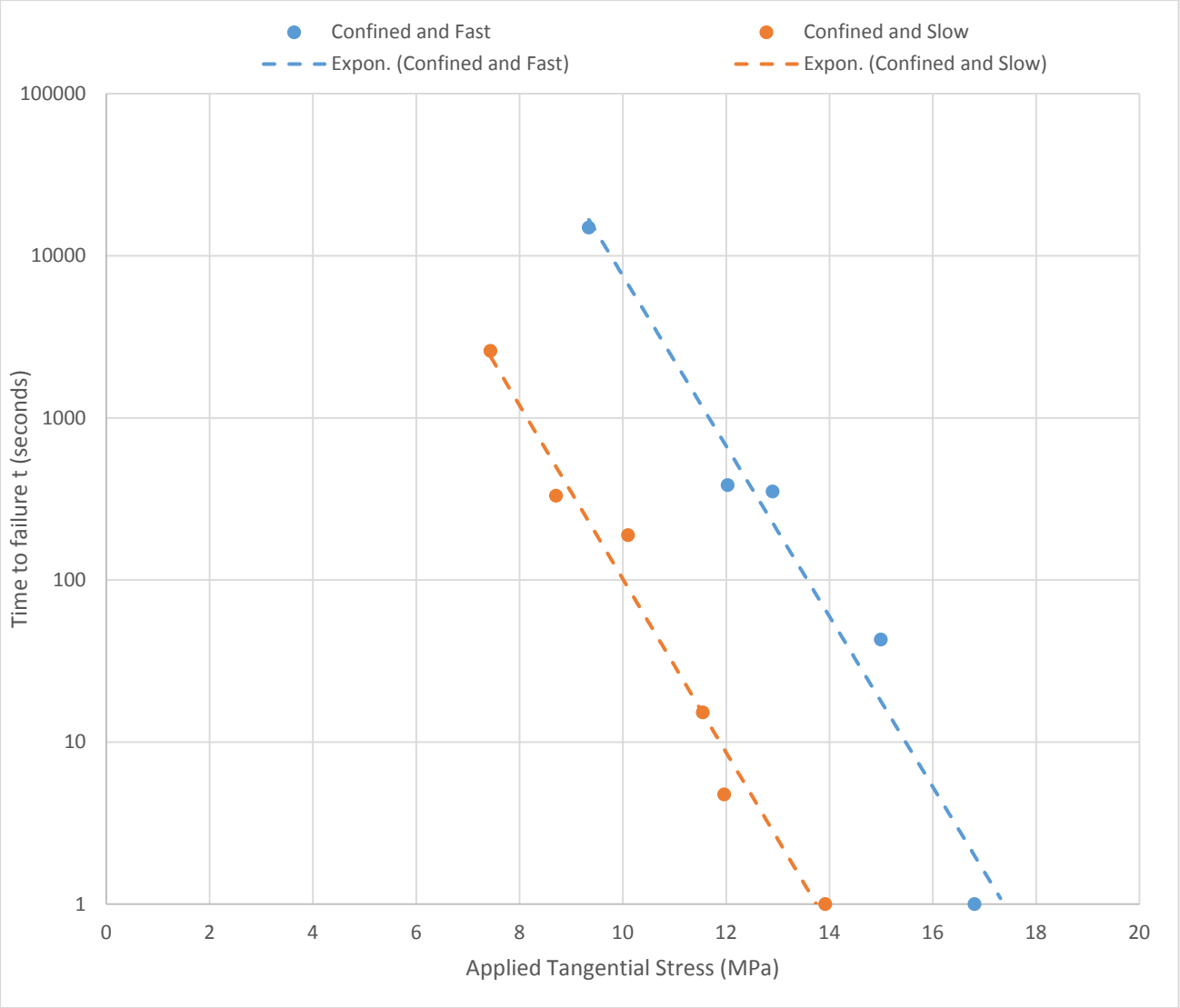

Figure 34: Comparison of the applied tangential stress for 'slow/penetrating' and 'fast/no penetration' cases with confining stress in sandstone. Theory predicts both value to be equal but a difference of ~3 MPa is noticeable.

5.1 DEPENDENCE OF β

Table 11: Comparison of β with viscosity

Fluid	Water in Latex Sheath	Glycerin	Soybean Oil	Water
Fluid penetration parameter β	1.00	1.23	1.32	2.02
Fluid Viscosity (Pa.s) at 20^0C	∞*	0.285	0.0635	0.001

*For the sake of this study, the latex sheath case is assumed to be a fluid with infinite viscosity.

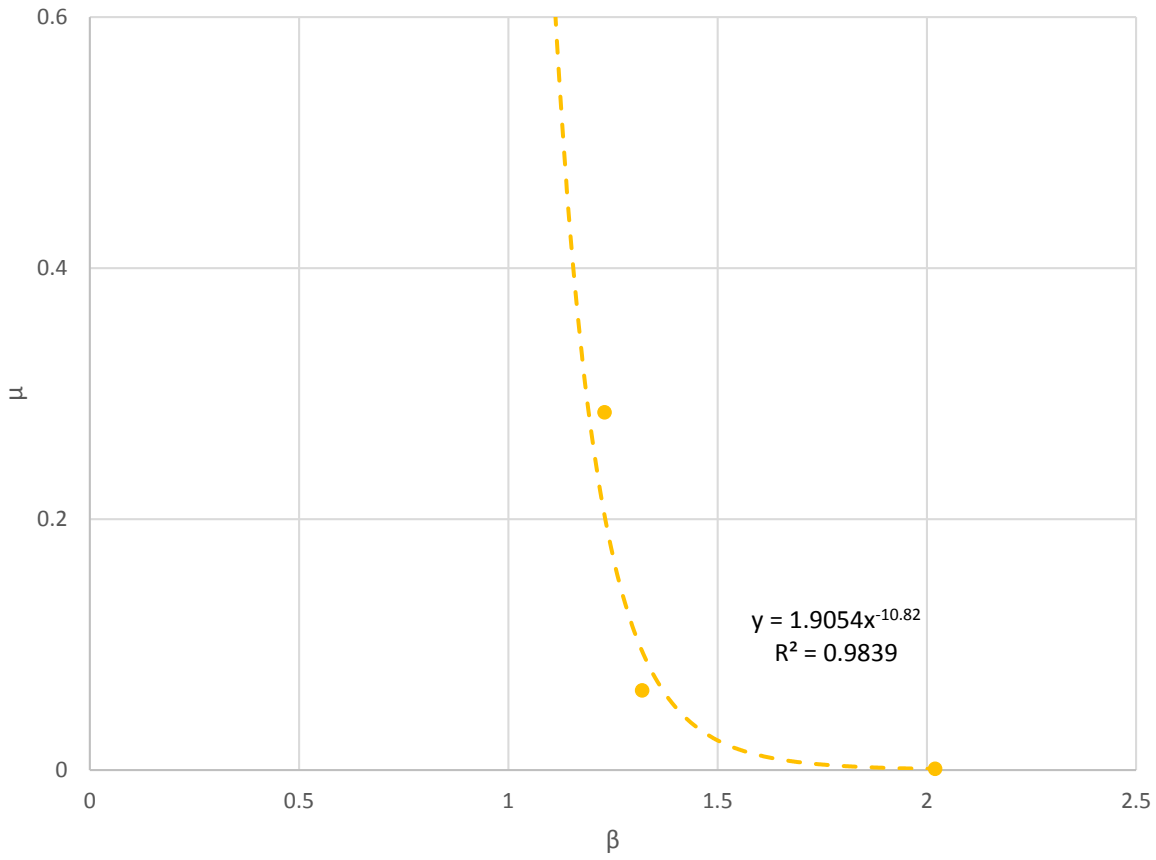

Figure 35: Viscosity at 20^0C vs Fluid Penetration parameter β for water, soybean oil and glycerin in sandstone.

Our plot suggests an exponential relationship between viscosity and fluid penetration, with viscosity approaching infinity as β approaches 1.

5.2 ROLE OF β

It is evident that fluids with moderate to high β values are a good choice in fracturing wells for initiating multiple fractures at low pressures.

Also using equation 1, knowledge of β as well as the rock tensile strength can help predict the breakdown pressure, or the other way around. Equation 1 is easily simplified by making $\hat{\sigma}$ equal to zero – by removing confining stress.

6.0 THE ROLE OF CONFINEMENT ON TIME-DEPENDENT INITIATION OF HYDRAULIC FRACTURES

Hubbert & Willis (1957) and Haimson & Fairhurst (1967) showed that the dependence of breakdown pressure on confining stress involved only a difference between both horizontal stresses and not the vertical stress. This is called the plane-strain model; and we have attempted to verify this theory experimentally.

To observe the role of confining stresses, we will compare cases of delayed breakdown with confinement and with no-confinement in sandstone (both $\beta = 1$ and $\beta = 2$) and in granite.

6.1 Confined vs Unconfined Delayed Breakdown in Sandstone ($\beta = 1$)

When we compare our 'fast' pressurization unconfined delayed breakdown experiments with those where confinement of σ_v, = 3.00 MPa, σ_H = 2.00 MPa and σ_h = 1.00 MPa was applied and apply the theory described in Chapter Two and evident in equation 5, we expect to see no change in the derivative of the relationship between pressure and time (marked by the slope) but only a rightward shift in the curve by a value of $\hat{\sigma} = 3\,\sigma_h - \sigma_H = 3(1) - 2 = 1$ MPa. We expect the relationship to be described by equation 6a and 6b below

$$t = A * \exp[(-\gamma) * (P_w)/kT] \qquad \text{(6a)} \quad \text{unconfined}$$

$$t = A * \exp[(-\gamma) * (P_w - 1\ \text{MPa})/kT] \qquad \text{(6b)} \quad \text{confined}$$

Even though we see no change of slope as expected. However, the rightward shift is much larger, a value of 6.6 MPa.

Table 12: Comparison of zero confinement case and a confinement case in no penetration delayed breakdown experiments in sandstone

Time (sec)	No Confinement Case Pressure (MPa)	Confinement Case Pressure (MPa)	Difference
10,000	3.8	10.6	6.80
1,000	5.7	12.2	6.50
100	7.7	14.2	6.50
10	9.6	16.2	6.60
1	11.4	18.2	6.80

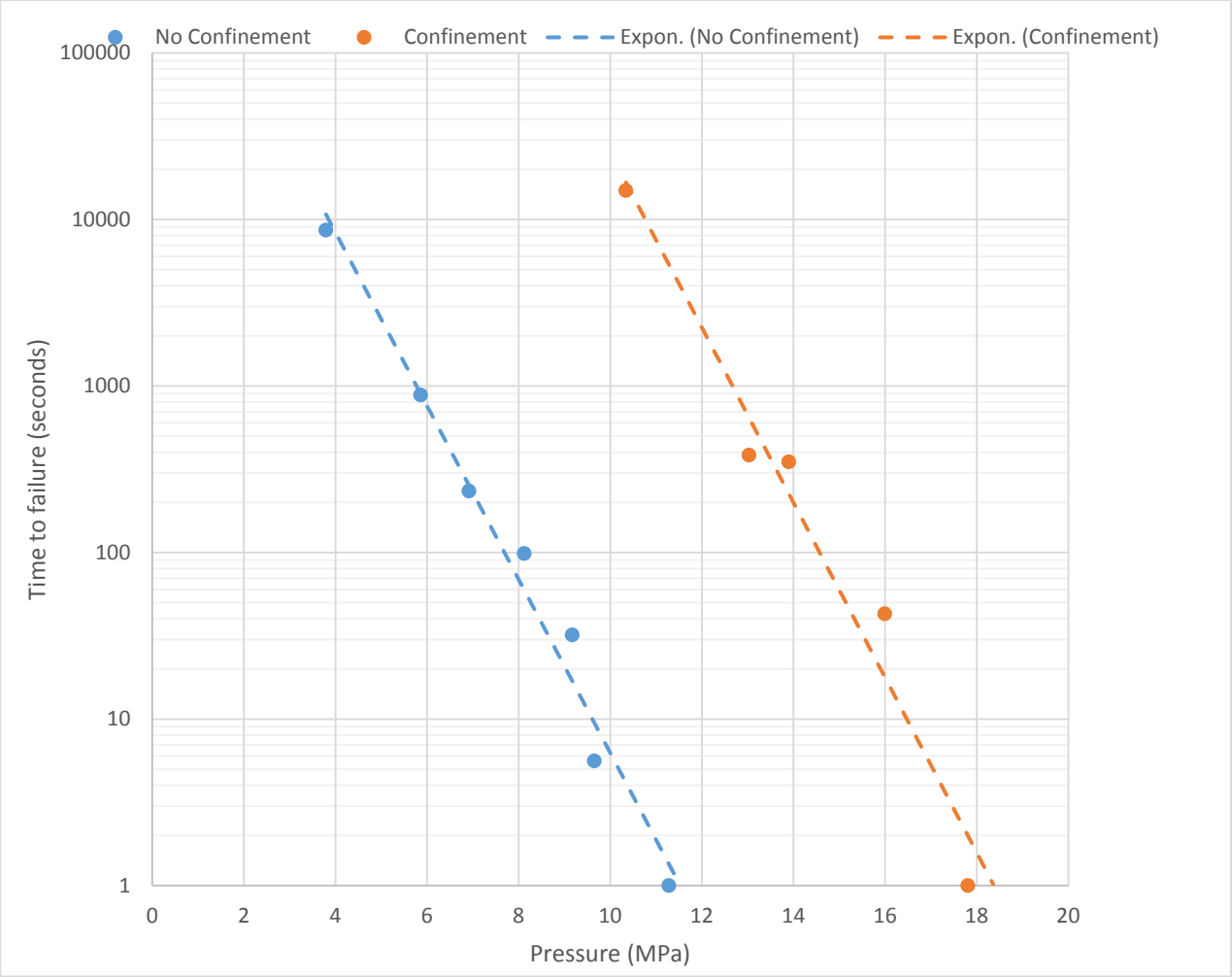

Figure 36: Curves for zero confinement case and a confinement case in no penetration delayed breakdown experiments in sandstone.

The larger than expected rightward shift can be explained, at least in principle, by the theoretical considerations of Detournay and Carbonell (1997). They showed that in the presence of confinement, rocks behave differently under 'slow' or penetrating conditions and 'fast' or non-penetrating conditions because initiation takes place from a small material flaw emanating from the wellbore. Using fracture mechanics, they showed that in the fluid penetration case, the fracture initiation pressure is usually equal to the breakdown pressure, as the energy for crack

propagation is lower than the energy for fracture initiation. This condition is marked by a negative rate of change of equilibrium pressure after initiation and unstable crack propagation. However, in the no fluid penetration case, the equilibrium pressure (that is the pressure for which a fracture mechanics propagation condition is just satisfied) continues to increase after fracture initiation because an increase in wellbore pressure is required for continued fracture propagation. When the crack is large, the equilibrium pressure is unbounded. This is called stable crack growth. This implies that the breakdown pressure recorded in the no fluid penetration case with confining stresses (orange curve in Figure 36), could be significantly larger than the fracture initiation pressure, even though both may be equal when there is fluid penetration.

Since the fracture was initiated prior to the point of instability referenced here as “breakdown”, the rightward shift of 6.6 MPa most likely is a result of additional energy required to overcome the confining stress and the energy required for stable crack propagation.

6.2 CONFINED VS UNCONFINED DELAYED BREAKDOWN IN SANDSTONE (β = 2)

For the cases of full fluid penetration, or 'slow' pressurization we compare our unconfined experiments and the confined ones, where the applied stresses were σ_v, = 3.00 MPa, σ_H = 2.00 MPa and σ_h = 1.00 MPa. We recall our equation 5, and expect the unconfined and confined cases to be described by equations 6c and 6d below respectively

$$t = A * \exp[(-\gamma) * (2P_w)/kT] \quad (6c) \qquad \text{unconfined}$$

$$t = A * \exp[(-\gamma) * (2P_w - \hat{\sigma})/kT] \qquad (6d) \quad \text{confined}$$

Therefore, if we plot time vs twice the breakdown pressure for unconfined and confined cases, we expect to see a similar slope, but a rightward shift by a value of $\hat{\sigma}$ = 3 $\sigma_h - \sigma_H = 3(1) - 2 = 1$ MPa. Our rightward shift is an average of 2.7 MPa.

Table 13: Comparison of zero confinement case and a confinement case in full penetration delayed breakdown experiments in sandstone

Time (sec)	No Confinement Case Pressure (MPa)	Confinement Case Pressure (MPa)	Difference ($\hat{\sigma}$)
10,000	2.7	7.2	4.5
1,000	5.0	9.0	4.0
100	7.6	10.8	3.2
10	9.6	12.6	3.0
1	12.0	14.4	2.4

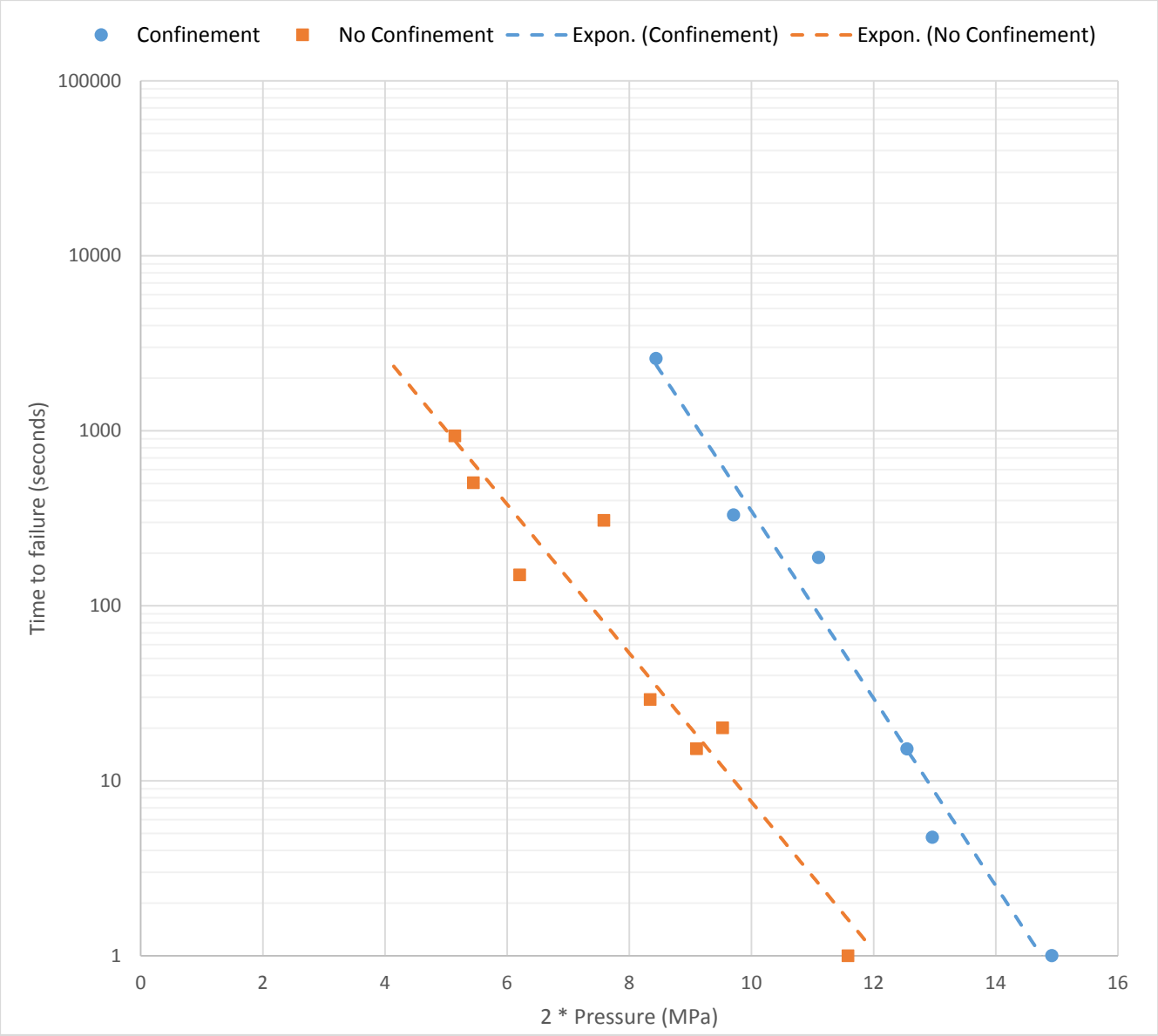

Figure 37: Curves for zero confinement case and a confinement case in no penetration delayed breakdown experiments in sandstone. A larger than expected shift is also recorded.

One noticeable trend is the marked deviation at longer times (t > 1000 seconds) especially in the penetration cases. This was discussed in Section 2.4 and related to Zhurkov neglecting the atomic scale bond reforming; only bond breaking is considered and at very low stresses, bond breaking and re-forming are in equilibrium. Hence our region of validity is at shorter times.

6.3 CONFINED VS UNCONFINED DELAYED BREAKDOWN IN GRANITE.

Before discussing the role of confinement, it is important to point out that results from unconfined charcoal granite show that material heterogeneity is high. This is observed during the fracture propagation phase. Whilst fracture propagation in sandstone shows minimal path deviation, path deviation is obvious in charcoal granite. The path deviation shows that the fracture chooses to grow along the ‘weaker’ spots in the material. This is likely caused by residual stresses in granite – an igneous rock formed by high pressure magma.

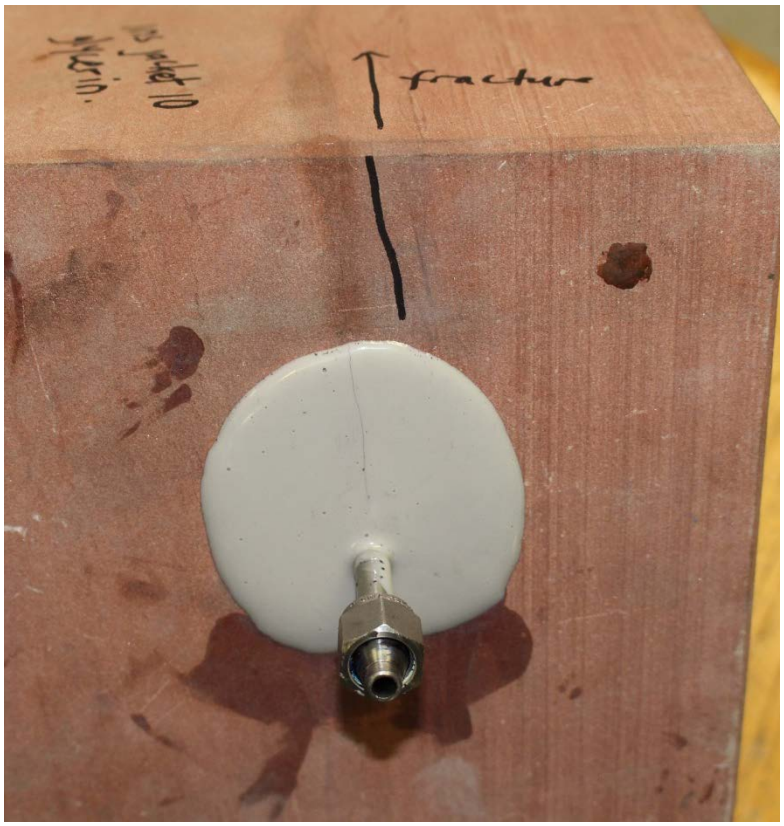

Figure 38: Fracture path in homogenous sandstone.

Figure 39: Fracture path in heterogeneous granite.

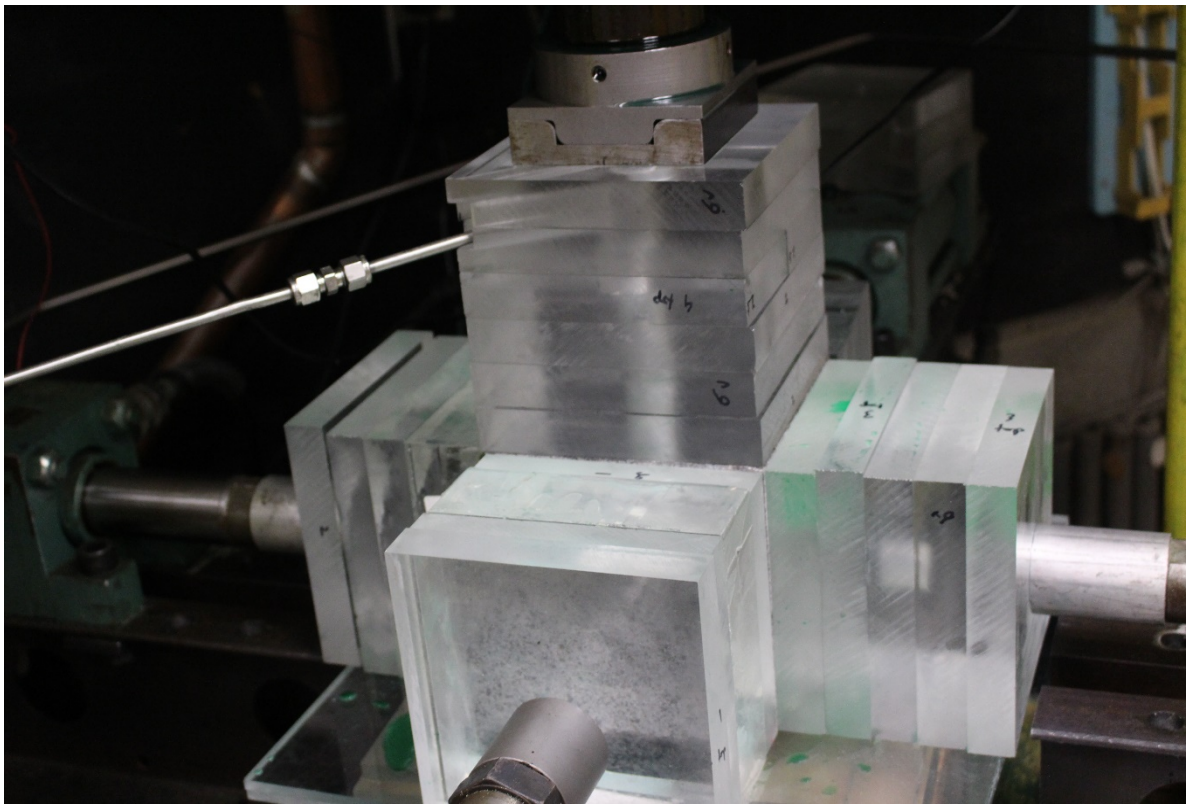

Figure 40: Set-up for confining stress experiment in charcoal granite

For an impermeable and non-porous rock, the value of β is close to 1. We carry this assumption into our experiments in granite. The delayed breakdown experiments in granite were performed using water as the fracturing fluid. In the case of zero confinement, the exponential relationship between pressure and time is clear. However, with confinement (σ_v, = 7.08 MPa, σ_H = 4.77 MPa and σ_h = 3.33 MPa), we see two exponential trends whose causation factor is traceable to experimental error. The leftward shift of five points between 14 – 16 MPa in Figure 41 represents experiments where minor damages to the rock occurred when applying the confining stress. The rock fabric damage was caused by pressure overshoot when targeting the set-point stress using the hydraulic pump regulator. Stress overshoot did occur in previous experiments on sandstone, but the magnitude of the overshoot was only able to cause rock damage in the granite (since we are testing at high confinement). Correction in stress application was done for the experiments around 14 MPa.

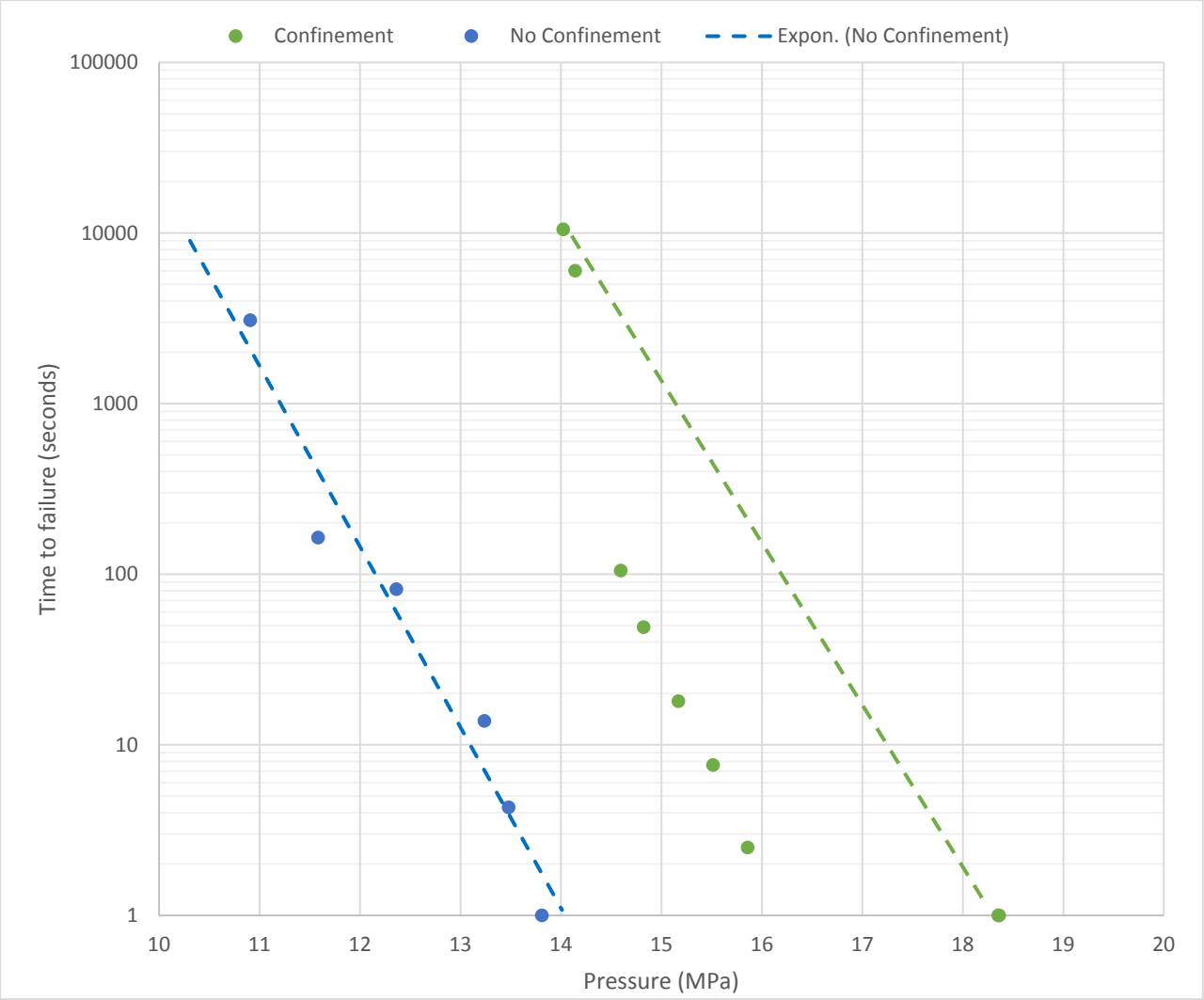

Figure 41: Curves for zero confinement case and a confinement case in partial penetration delayed breakdown experiments in charcoal granite.

If we assume $\beta \sim 1$, then the applied stress ($\sigma_{\theta\theta}^{(max)}$) is equal to the applied pressure P_w since ($\sigma_{\theta\theta}^{(max)} = \beta P_w - \hat{\sigma}$). Therefore if we plot time vs breakdown pressure for the case of confinement ($\hat{\sigma} = 3\,\sigma_h - \sigma_H = 3(3.3) - 4.7 = 5.2$) alongside the case of no-confinement ($\hat{\sigma} = 0$) the plane-strain theory predicts the curve to shift rightward by an arithmetic value of 5.2 MPa. If we assume the leftward shift is due to rock fabric damage and draw the trendline using

the four extreme points (two instantaneous breakdown points overlapping, and the delayed breakdown at 14.0 and 14.1 MPa), then the shift ($\hat{\sigma}$) value is circa 4.5 MPa which is quite close with the predicted value.

7.0 CONCLUSIONS.

Hydraulic fracturing experiments where there is no fluid penetration have been successfully carried out and following classical hydraulic fracturing theory prediction, the breakdown pressure is shown to be equal to the material tensile strength. In addition, the occurrence of delayed initiation at lower pressures indicates that sub-critical fracture initiation/breakdown is possible and there is a clear, theoretically-predicted exponential relationship between the applied pressure and the time for initiation. This exponential relationship has been shown in sandstone, for ‘slow’ and ‘fast’ pressurization and at zero and low confining stress values. In granite, it has been shown for partial fluid penetration and high confining stresses. The impact of rock damage due to stress overshoot during application was also observed in granite.

In summary, then, the main contribution of this thesis is threefold:

Firstly, it provides the first comprehensive validation of the exponential relationship between initiation/breakdown time and applied wellbore pressure, with confinement and no/partial/full fluid penetration. This relationship was predicted theoretically by Bunger and Lu (2015) and preliminary experimental support by a series of unconfined experiments in granite using glycerin as the driving fluid, was described by Lu et al. (2015).

Secondly, this thesis provides perhaps the clearest demonstration of the impact of fluid penetration on hydraulic fracture initiation/breakdown. The impact of fluid penetration is evident in the experimental results. Most strikingly the pressure required for breakdown, whether instantaneously or after a delayed time, in a full fluid penetration case has been shown to be half that in a no-fluid penetration case. This factor of two difference between the full penetration and non-penetrating end members means these results are consistent with Hubbert & Willis (1957) in the non-penetrating cases, Haimson & Fairhurst (1967) in the fully penetrating cases, with resolution in terms of degree of penetration ("fast" and "slow" penetration) as proposed by Detournay and Carbonell (1997). Practically, then, lower viscosity fluids are expected to reduce the pressure requirement for the initiation/breakdown portion of hydraulic fracturing treatments. Also, by quantifying the fluid penetration parameter β and demonstrating its impact, these experiments confirm the possibility suggested by Bunger and Lu (2015) to design stimulations so that multiple fracture initiation is promoted by the evolving value of β (owing to the first fractures to initiate under "fast" pressurization conditions with little fluid penetration and later fractures to initiation under "slow" pressurization conditions, with large fluid penetration.

Finally, this thesis shows the impact of confining stresses, ubiquitously present at depth, on delayed initiation/breakdown of hydraulic fractures. For penetrating fluids, the role of confining stresses observed in the experiments is fairly consistent with the predictions of Bunger and Lu (2015). For jacketed experiments with zero penetration, the confining stress increases has a much stronger impact on the breakdown pressure than predicted by theory, giving rise to a need for theory that accounts for the evolution of fracture growth up to the point of instability in these non-penetrating cases.

These experiments give rise to several ongoing questions for investigation. As previously mentioned, the onset of instability in jacketed experiments should be examined theoretically and, complimentary to this study, would be a series of experiments more closely examining this instability through detection of acoustic emission (AE) generated and/or through direct observation of growth in transparent materials.

Additionally, more independent measurement of static fatigue and subcritical crack growth properties will strengthen the validation the experiments provide to the theory. These measurements can be provided by three-point and four-point bending test, indirect tension tests, and double-torsion tests.

Finally, extension of the results to a wider range of confining stresses, penetration conditions, and rock types will enhance the validation of the theory and undoubtedly illuminate conditions under which the theory is inadequate. Suggested additional tests include full-penetration and no-penetration cases at different values of σ_v, σ_H and $\sigma_h$whilst retaining the same value of $\hat{\sigma}$. The behavior under higher values of these stresses can also be investigated using materials of adequate strength, thereby minimizing wellbore damage due to the loading. On the same topic, quantifying the induced wellbore damage and its impact is also an important area of future investigation. More studies should also be done on fluid penetration, by conducting similar experiments using other fluids, as well as deriving values of β and exploring the relationship between β and the hydraulic conductivity. The role of penetrating fluids in decreasing the rock's resistance to fracturing should also be clarified, especially for rocks that are known to be sensitive to fluid chemistry such as limestone and shale.

APPENDIX A

RAW PRESSURE VS TIME AND FLOWRATE VS TIME RECORDS FOR SELECTED EXPERIMENTS

(i) Pressure record for 850 psi delayed breakdown with no fluid penetration and no confining stresses.

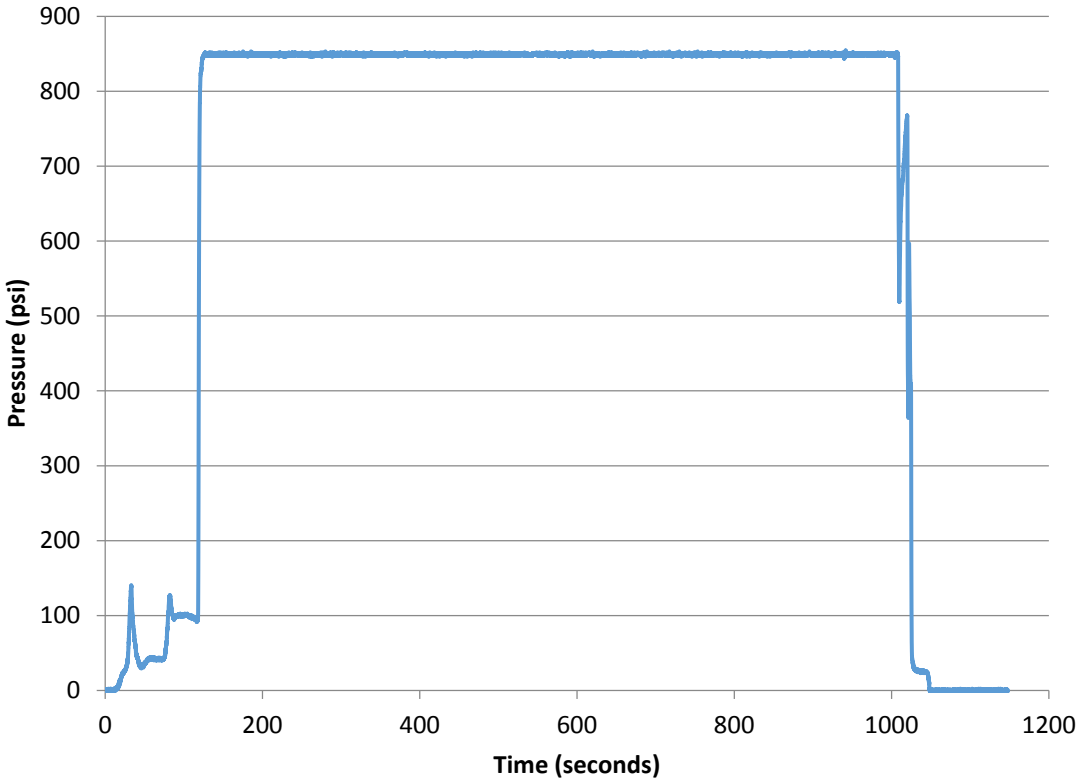

(ii) Flowrate record for 850 psi delayed breakdown with no fluid penetration and no confining stresses.

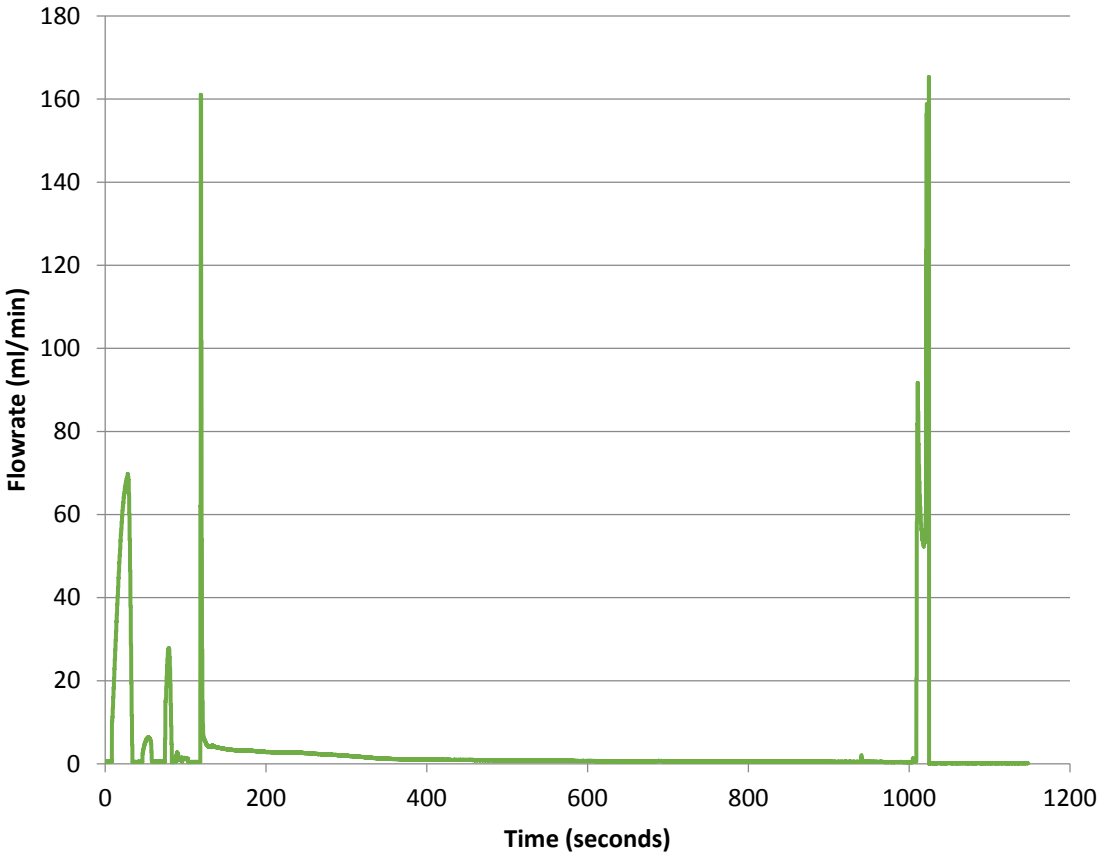

(iii) Pressure record for Instantaneous breakdown with no fluid penetration and no confinement

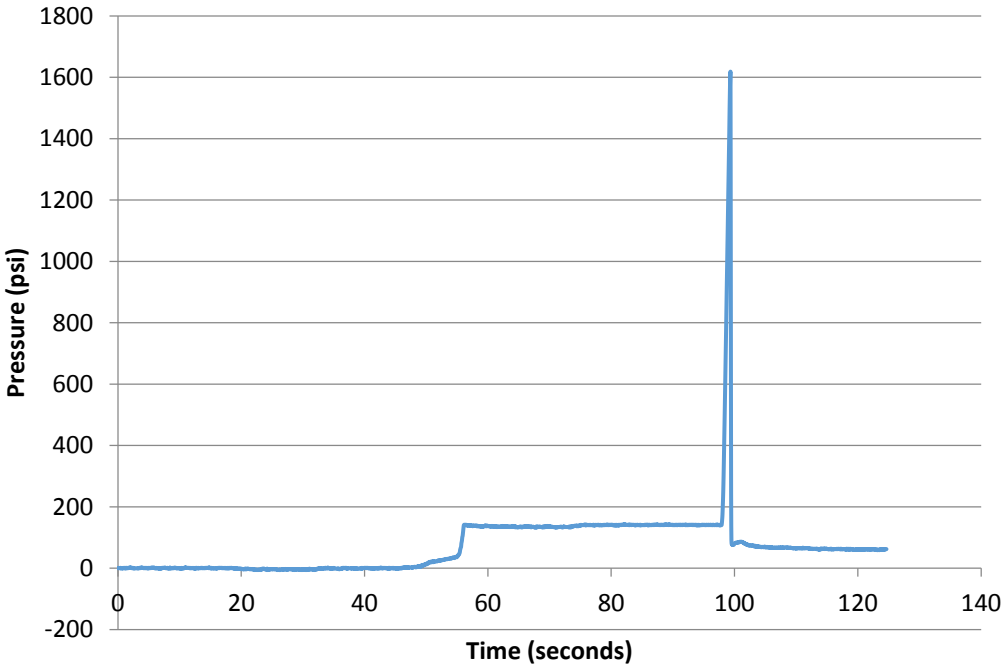

(iv) Flowrate record for Instantaneous breakdown with no fluid penetration and no confinement

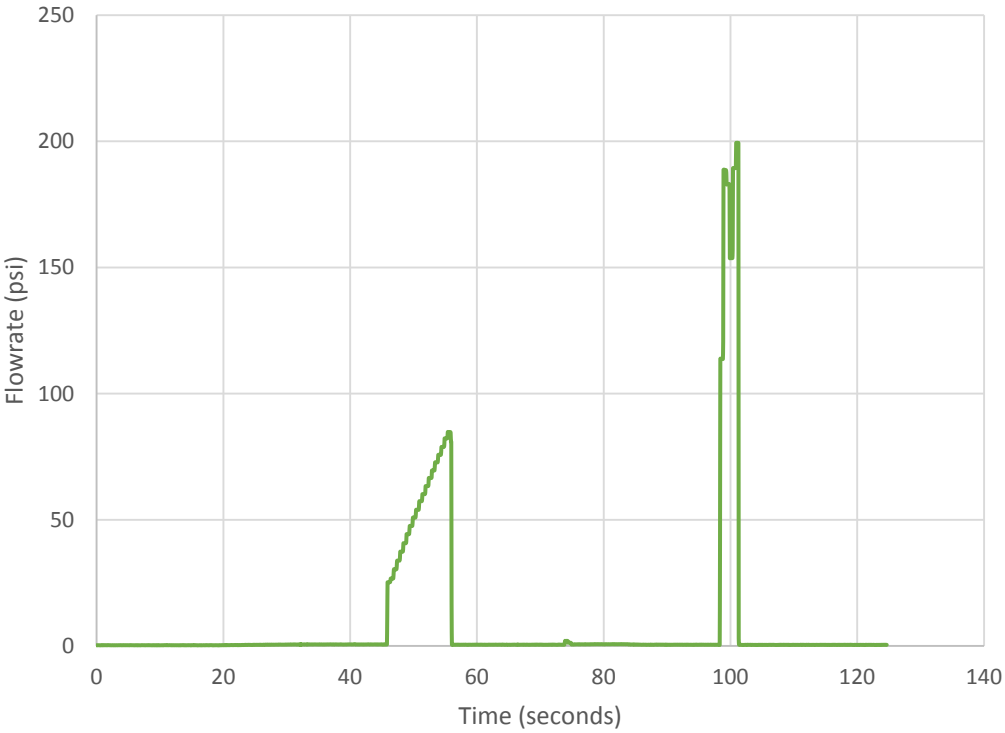

(v) Pressure record for 610 psi delayed breakdown with full fluid penetration and zero confinement

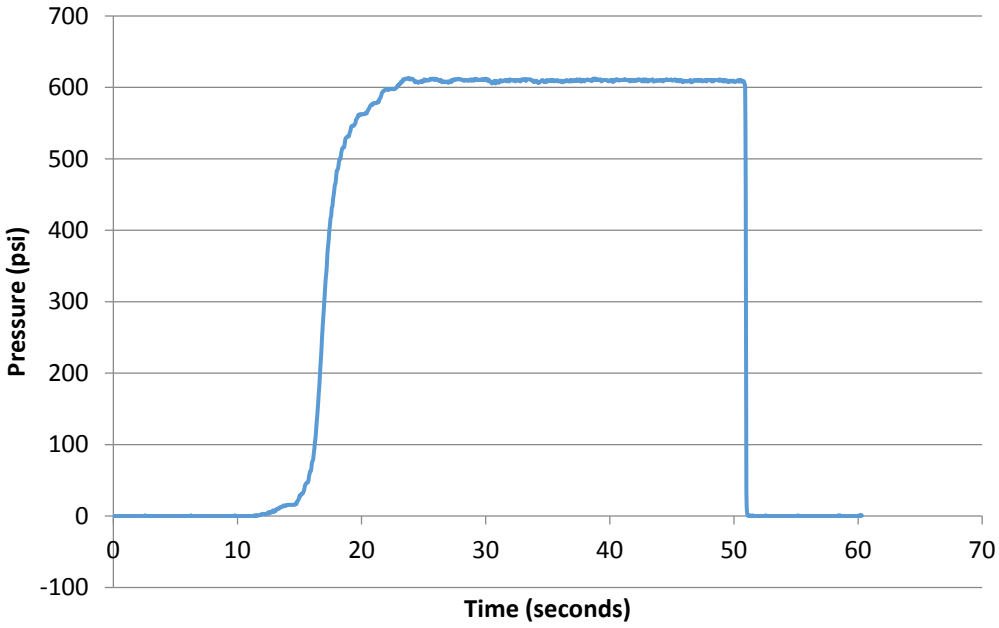

(vi) Flowrate record for 610 psi delayed breakdown with full fluid penetration and zero confinement

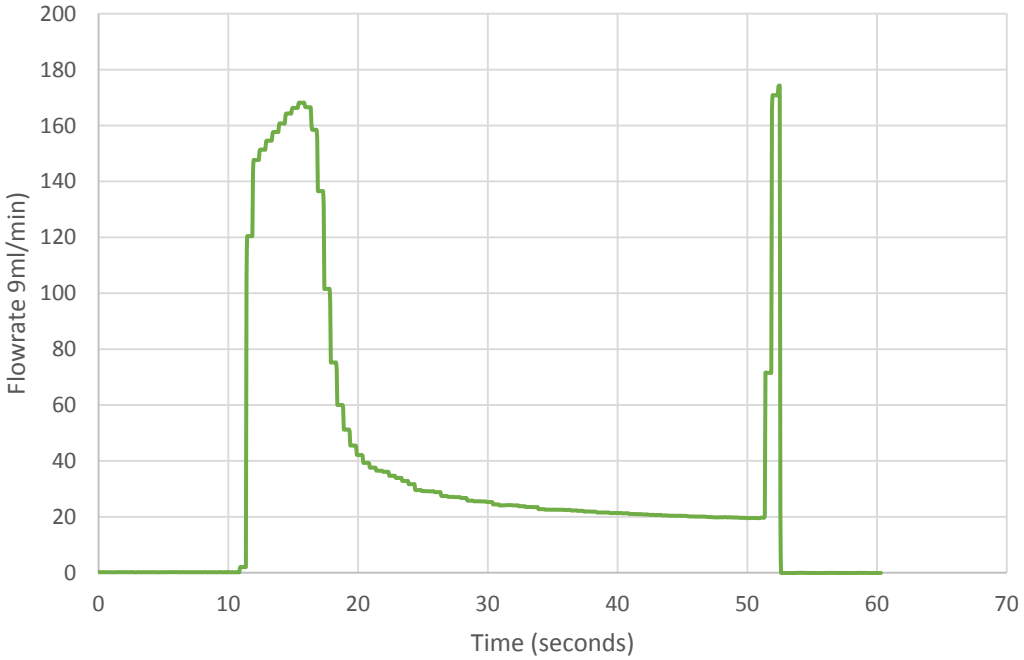

(vii) Pressure record for 2016 psi delayed breakdown with no fluid penetration and confining stresses of 1,2 and 3 MPa

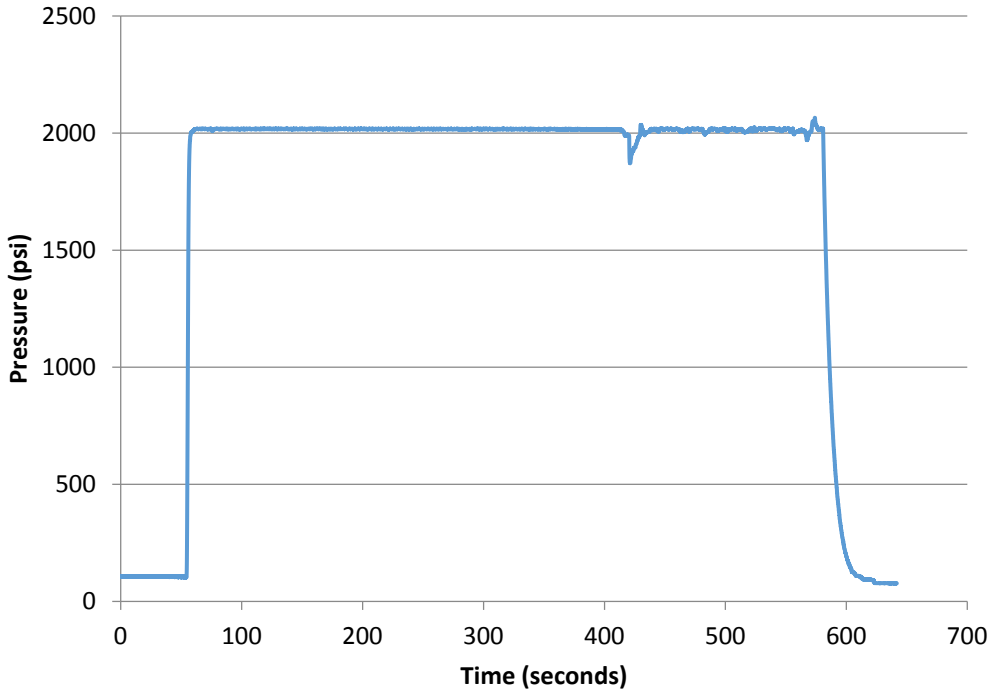

(viii) Pressure record for 2016 psi delayed breakdown with no fluid penetration and confining stresses of 1,2 and 3 MPa

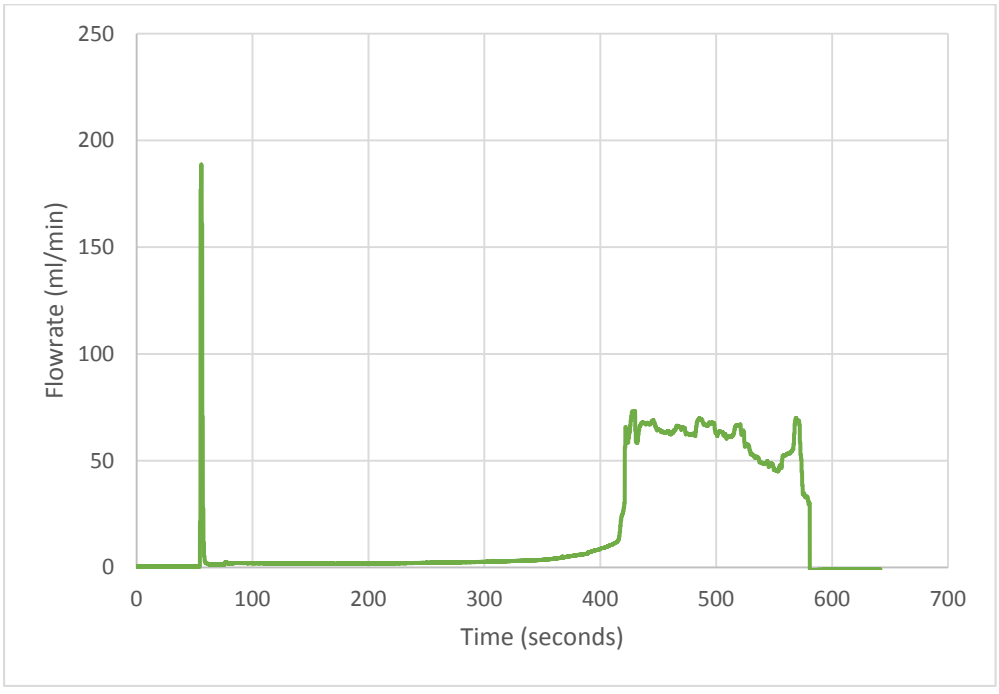

(ix) Confining stress record for 2016 psi delayed breakdown with no fluid penetration and confining stresses of 1,2 and 3 MPa

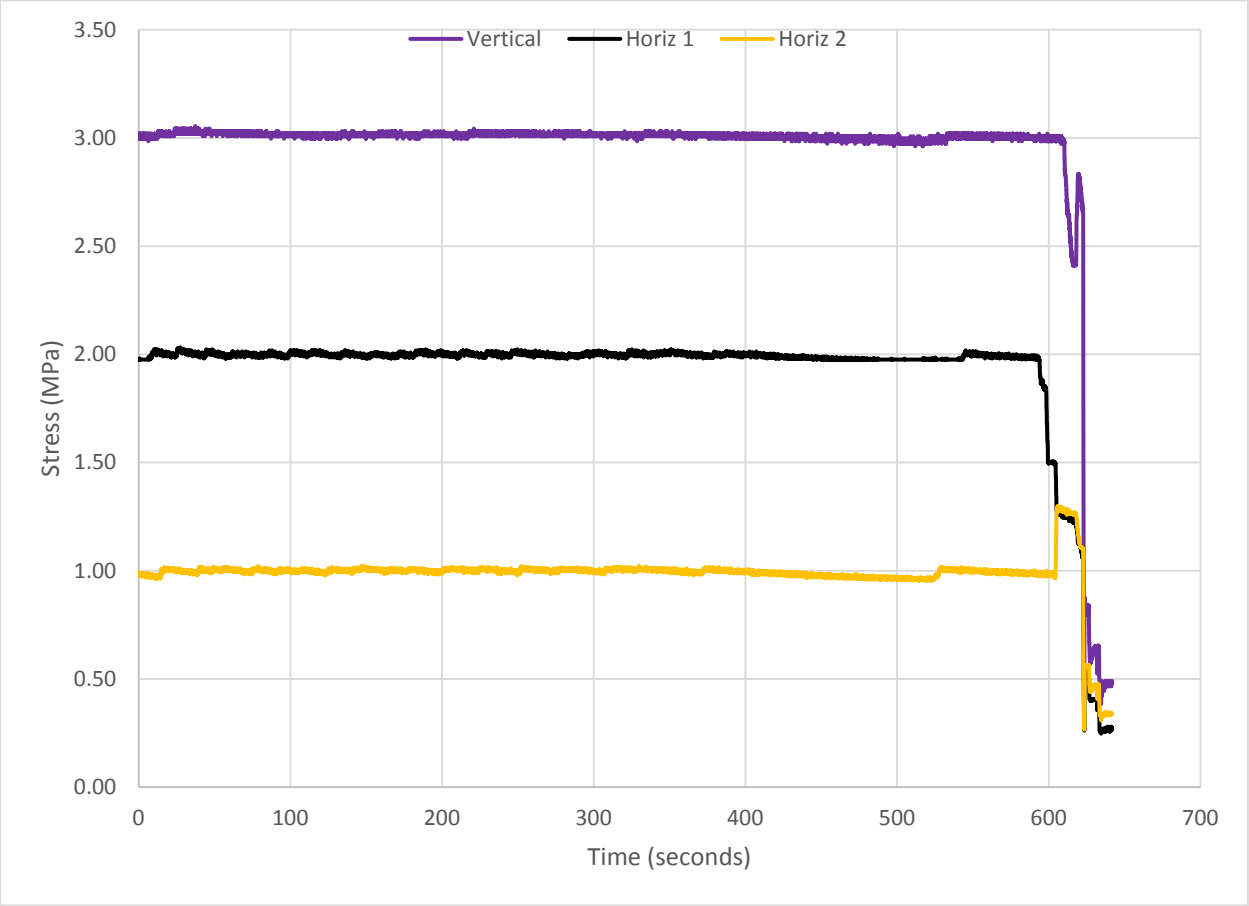

(x) Pressure record for Instantaneous breakdown with full fluid penetration and confining stresses of 1,2 and 3 MPa

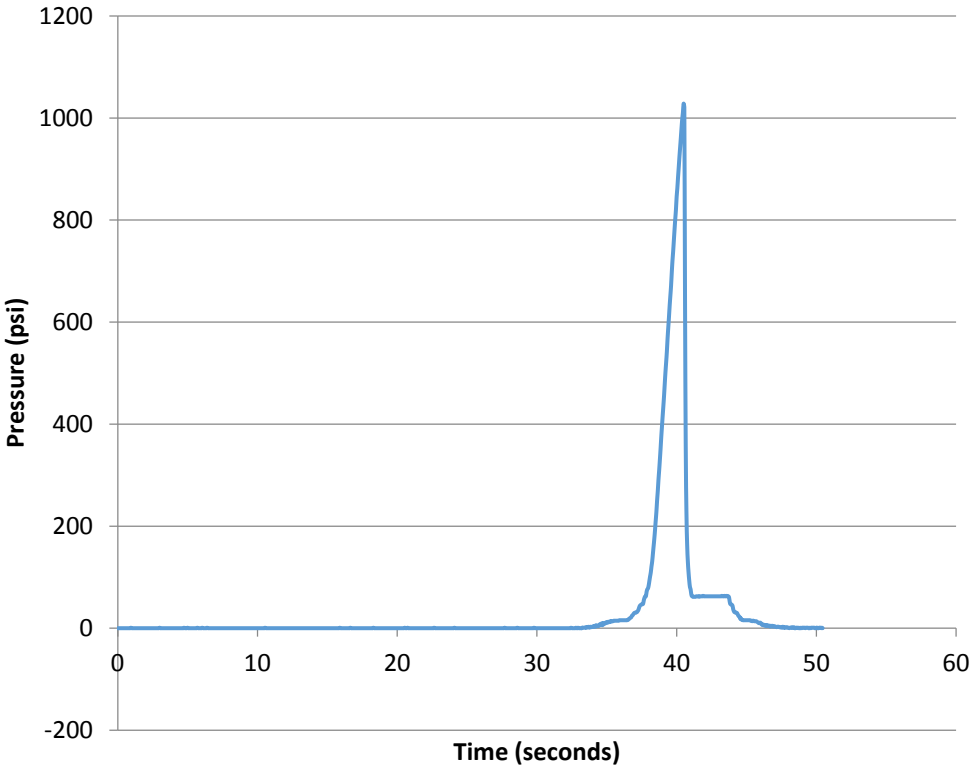

(xi) Flowrate record for Instantaneous breakdown with full fluid penetration and confining stresses of 1,2 and 3 MPa

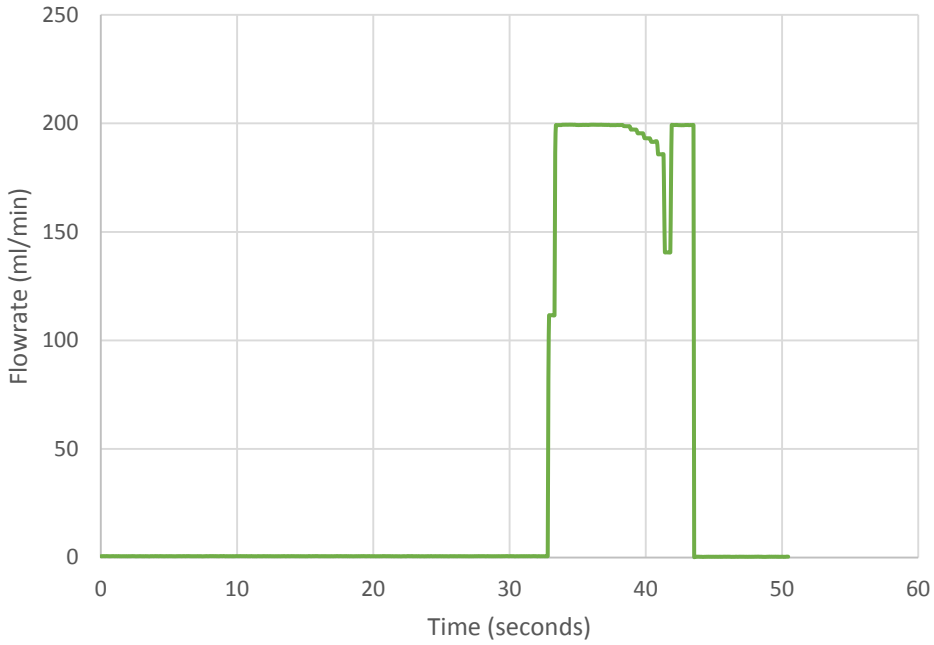

(xii) Confining stress record for Instantaneous breakdown with full fluid penetration and confining stresses of 1,2 and 3 MPa

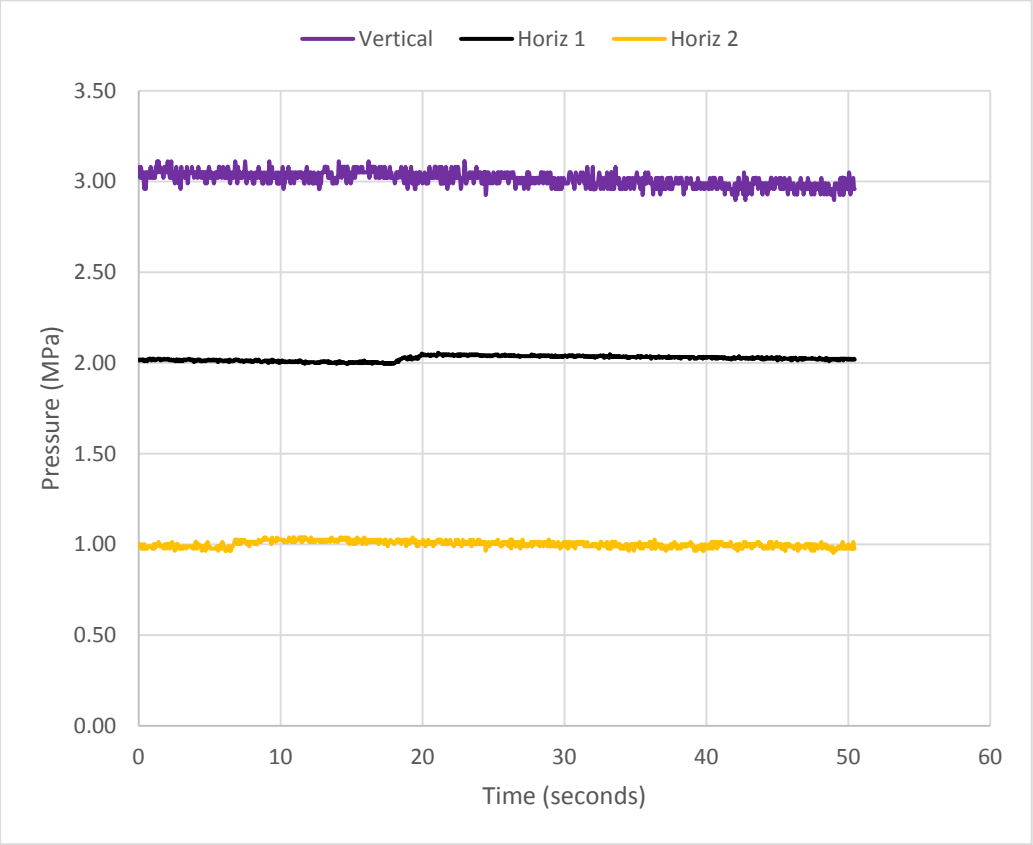

APPENDIX B

ADDITIONAL PHOTOGRAPHS OF EXPERIMENTS

(i) Charcoal granite cross section after breakdown

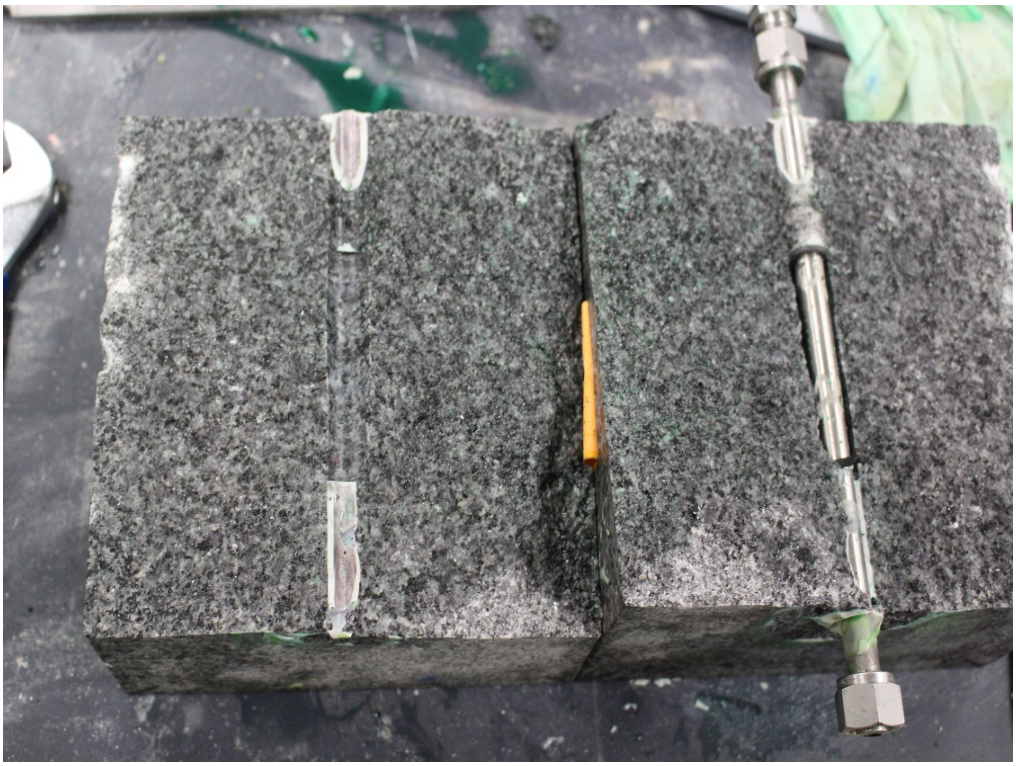

(ii) Charcoal granite, during test

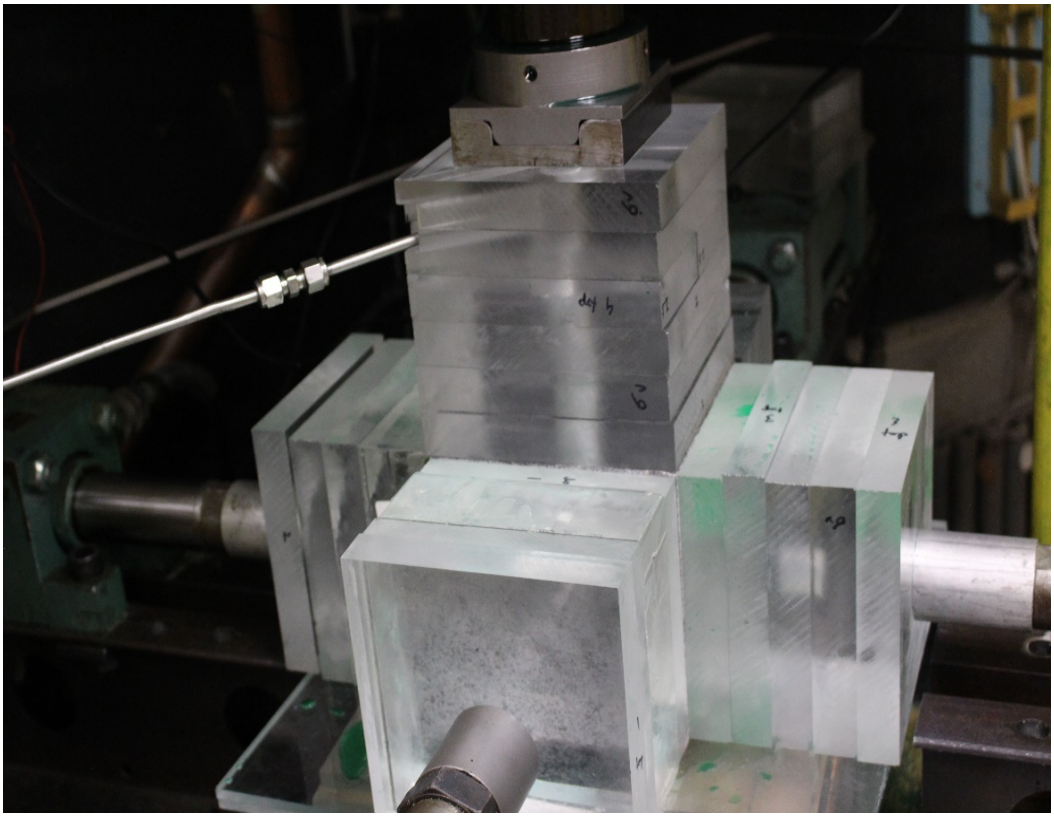

(iii) Sandstone no penetration case with confinement after fracturing

(iv) Sandstone block during testing

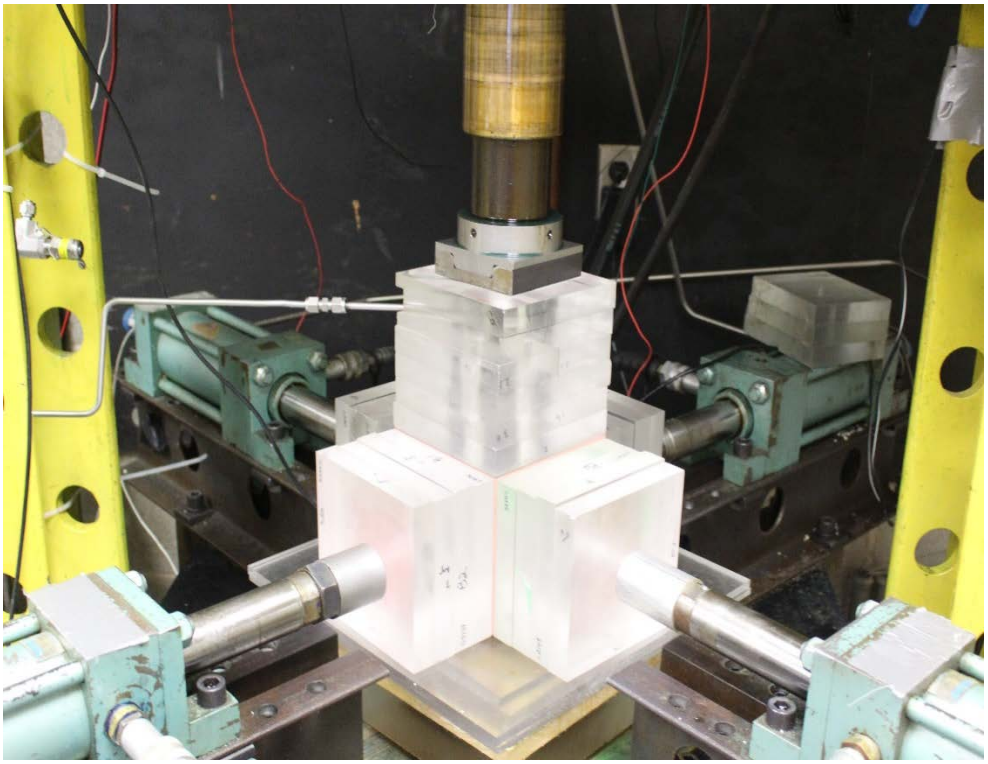

(v) Mapping fracture path in charcoal granite by pumping air into wellbore after experiment

(vi) Front view of sandstone after fracturing with water

REFERENCES

1. Bunger AP, Lu G. In Press. Time-Dependent Initiation of Multiple Hydraulic Fractures in a Formation with Varying Stresses. SPE Journal. Accepted 20 March 2015. http://dx.doi.org/10.2118/171030-PA.

2. Detournay, E. and Cheng, A.H.-D., "Fundamentals of poroelasticity," Chapter 5 in Comprehensive Rock Engineering: Principles, Practice and Projects, Vol. II, Analysis and Design Method, ed. C. Fairhurst, Pergamon Press, pp. 113-171, 1993.

3. Detournay, E. and R. Carbonell, 1997: "Fracture mechanics analysis of the breakdown process in minifracture or leakoff test". SPE Prod & Fac 12 (3): 195-199.

4. Economides and Nolte, 2000: Reservoir Stimulation. Wiley 3rd Edition.

5. Haimson, B. and C. Fairhurst, 1967: "Initiation and extension of hydraulic fractures in rocks". SPE Jour. 7 (3): 310-318.

6. Haimson, B. and C. Fairhurst, 1969: "Hydraulic fracturing in porous-permeable materials". Journal of Petroleum Technology, July 1969: 811-817.

7. Haimson. 1968: "Hydraulic fracturing in porous and nonporous rock and its potential for determining in-situ stresses at great depths". PhD Dissertation, University of Minnesota

8. Hubbert, M. and D. Willis. 1957: "Mechanics of hydraulic fracturing". Trans. AIME. 210: 153–168.

9. Kear, J. and A.P. Bunger, 2014: "Dependence of static fatigue tests on experimental configuration for a crystalline rock". Advanced Materials Research, 891: 863–871.

10. Lakirouhani, A., A.P. Bunger, and E Detournay. 2008: "Modeling initiation of hydraulic fractures from a wellbore". In Proceedings, 5th Asian Rock Mechanics Symposium, Tehran, Iran, 24-26 November: 1101–1108.

11. Lu, G., Uwaifo, E. C., Ames, B. C., Ufondu, A., Bunger, A. P., Prioul, R., Aidagulov, G. 2015: "Experimental Demonstration of Delayed Initiation of Hydraulic Fractures below Breakdown Pressure in Granite". 49th U.S. Rock Mechanics Symposium. San Francisco, CA, USA. Paper No. 15-190.

12. Nolte, 2000: Evolution of Hydraulic Fracturing Design and Evaluation, Appendix 5-1, Economides and Nolte, 2000: Reservoir Stimulation. Wiley 3rd Edition.

13. U.S. Department of Energy, Energy Information Administration, 2015: World Shale Resource Assessments. Retrieved from http://www.eia.gov/analysis/studies/worldshalegas/

14. Walker K.J., Wutherich J., Terry I., Shreves J.E., Caplan J. 2012: "Improving Production in the Marcellus Shale Using an Engineered Completion Design: A Case Study". SPE Annual Technical Conference and Exhibition, 8-10 October, San Antonio, Texas, USA. SPE-159666-MS

15. Yoxtheimer, 2013 Water Recycling ─ a Staple in the Marcellus Shale. www.shaleplaywatermanagement.com.

16. Zhurkov, S. N. 1984: "Kinetic concept of the strength of solids". Int. J. Fracture. 26 (4): 295–307.